UNIVERSITÉ DE MONTRÉAL

EFFECTS OF CONCEALED CONDUCTION ON AV NODAL FUNCTION

PAR

BOCHUN XU

DÉPARTEMENT DE PHYSIOLOGIE

FACULTÉ DE MÉDECINE

MÉMOIRE PRÉSENTÉ À LA FACULTÉ DES ÉTUDES SUPÉRIEURES EN VUE DE L'OBTENTION DU GRADE DE MAÎTRISE EN PHYSIOLOGIE

SEPTEMBRE 2005

Université de Montréal

Faculté des études supérieures

Mémoire intitulé :

EFFECTS OF CONCEALED CONDUCTION

ON AV NODAL FUNCTION

ou

EFFETS DE LA CONDUCTION CACHÉE

SUR LA FONCTION DU NOEUD AV

Présenté par :

Bochun Xu

Évalué par un jury composé des personnes suivantes :

Dr Réjean Couture, président rapporteur

Dr Jacques Billette, directeur de recherche

Dr René Cardinal, membre

RÉSUMÉ

Bien-fondé: Les principes et le substrat soustendant la conduction cachée dans la double voie de conduction du nœud auriculoventriculaire (AV) demeurent mal compris.

Objectif: Déterminer comment les propriétés de conduction cachée du noeud AV se développent dans ses voies lente et rapide.

Méthodes: La zone de conduction cachée et les effets de cycles choisis dans cette zone sur les courbes de fonction nodale ont été déterminés avec et sans un cycle conditionnant (10 ms plus long que la période réfractaire efficace et inséré avant le cycle caché) avant et après l'ablation de la voie lente dans 6 préparations de cœur de lapin.

Résulats: Étroite et inconsistante (22±12 ms, n=3) lorsque déterminée avec un battement caché seul, la zone de conduction cachée est devenue large et consistante (77±47 ms, n=6, $p<0.03$) quand un battement conditionnel conduit précédait le battement caché. La période réfractaire efficace et fonctionnelle du nœud AV s'allongèrent en proportion de la longueur du cycle caché qui déplaça toute la courbe de récupération (voies lente et rapide) vers la droite sans en changer la morphologie. En d'autres mots, tout battement caché réinitialise le cycle de récupération dans les deux voies. L'ablation de la voie lente a aussi élargi et rendu consistante la zone de conduction cachée sans altérer la réponse résultante de la voie rapide. Un battement caché dans une voie lente interrompue continue d'affecter la courbe de la voie rapide à toutes les longueurs de cycle.

Conclusions: Une large zone de conduction cachée est une propriété consistante du nœud AV. Le cycle conditionnant seul ou combiné à une ablation de la voie lente en facilite l'expression. La réinitialisation du cycle d'excitabilité dans les voies lente et rapide sont responsables pour la conduction cachée.

Mots clefs: Voie lente, voie rapide, conduction, état réfractaire, modulation électrotonique

ABSTRACT

Background: The rules and substrate underlying concealed conduction in atrioventricular (AV) nodal dual pathways remain unclear.

Objective: Determine how the concealed conduction properties of the AV node develop in its slow and fast pathway.

Methods: The nodal concealment zone and effects of increasing concealed cycle lengths chosen within the concealment zone on nodal function curves were determined with and without a conditioning cycle (10 ms longer than ERPN) before and after slow pathway ablation in 6 rabbit heart preparations.

Results: From narrow and inconsistent (22±12 ms, n=3) when determined with a blocked beat, the concealment zone became broad and consistent (77±47 ms, n=6, $p<0.03$) when determined with a blocked beat preceded by a conducted conditioning beat. The increase in the concealed cycle length resulted in proportional ERPN and FRPN (effective and functional refractory period of AV nod) prolongation and rightward shift of the entire nodal recovery curve (slow and fast pathway) to a longer atrial cycle length range without affecting the curve shape. In other words, any concealed beat resets the whole recovery process in both pathways. The slow pathway ablation also broadened and made the concealment zone consistent but did not alter the fast pathway responses to concealed conduction. A beat concealed in interrupted slow pathway still alters fast pathway curve at all cycle lengths.

Conclusions: A broad concealment zone is a consistent nodal feature. A conditioning cycle and/or slow pathway ablation favor its expression. Reset excitability cycle in the slow and fast pathway accounts for the effects of concealed AV nodal conduction.

Keywords: Slow pathway, fast pathway, conduction, refractoriness, electrotonic modulation

TABLE OF CONTENTS

LIST OF FIGURES

CHAPTER I

CHAPTER II

CHAPTER III

LIST OF ABBREVIATIONS

AV	=	atrioventricular
AN	=	atrionodal
N	=	nodal
NH	=	nodal-His
RR	=	interval between two electrocardiographic R waves
ERPN	=	effective refractory period of AV node
FRPN	=	functional refractory period of AV node
AA	=	atrial interval
HA	=	His-atrial interval
AVNRT	=	AV nodal reentrant tachycardia

ACKNOWLEDGMENTS

I would like to thank all peoples who contributed to make this thesis possible and an enjoyable experience for me.

First, I wish to express my sincere gratitude to my thesis director, Dr. Jacques Billette, who guided this work and was easily available to help. His understanding, encouragement, support, and friendship help are especially appreciated. His scientific spirit and attitude of creativeness, rigors, as well as hard-working have impelled me to pursue my program in the past three years and will continuously influence my future career.

Sincere thanks are also extended to:

Mr. Maurice Tremblay, for his expert assistance throughout my training, for his contributions to this work, and particularly, for providing us an enjoyable atmosphere.

Mrs. Lise Plamondon, for her skilful hands in assisting experiments and in preparing graphic illustrations, and for being so friendly all which made it so pleasant to work with her.

Finally, I would like to express my deepest gratitude for the constant support, understanding and love that I received from my husband, Mr. Fang Guan and my parents during the past years.

INTRODUCTION

The AV node plays a strategic role in both normal and arrhythmic cardiac activation. It generates a delay between atrial and ventricular activation that favors ventricular filling and effective blood pumping. It also filters impulses during supraventricular tachyarrhythmias to maintain a cycle length compatible with blood pumping. Since its discovery by Tawara,[1] it has been the object of much study by a number of investigators both at the cellular and organ level. Despite important progresses made in the understanding of its anatomy, electrophysiology, and functional properties, the AV node remains puzzling in many respects.[2] Zipes[3] elegantly summarized the problem by suggesting that "the AV node is a riddle wrapped in a mystery inside an enigma". Despite important limitations in its understanding, the AV node remains a primary target of antiarrhythmic therapy. Amongst others, ablation therapy for the most frequent clinical arrhythmia called AV nodal reentrant tachycardia has greatly developed to become a success story in cardiology with a success rate of nearly 100%.[4,5] Paradoxically, the dual pathway substrate underlying this arrhythmia remains highly debated both in terms of anatomy and physiology. The present study concerns a problem related to this dual pathway substrate. To better understand this problem let us first recall briefly some basic notions of AV nodal physiology.

Unlike the other portions of the AV conduction system where the speed of conduction is generally constant from beat to beat, the conduction speed in the AV node is highly variable. The resulting AV nodal delay, referred to as nodal conduction time in this thesis, can vary markedly in responses to changes in autonomic tone,[6,7] intrinsic properties[8-10] or both. The functional state of the AV node is particularly sensitive to

changes of heart rate that may result in a wide variety of responses even in the presence of a constant autonomic tone. This intrinsic rate-dependent behavior of AV node obeys 3 basic functional rules known as recovery, facilitation and fatigue.[8,9,11-14] Recovery refers to the increase in nodal conduction time with shortening of preceding cycle length. For a constant fast rate, the nodal conduction time increases with time and rate, a property called fatigue. For a constant recovery time and rate, nodal conduction time decreases in short recovery time range with the preceding cycle length, a property called facilitation. There is also increasing evidence that the normal AV node has a fast and a slow pathway.[15-19] Recent studies suggest in fact that the slow and fast pathway have each their own set of rate-dependent properties so that the overall rate-dependent properties of the node would reflect their net sum.

Amongst communally observed rate-induced AV nodal responses is the one to atrial fibrillation, the most common sustained supraventricular tachyarrhythmias. In patient with atrial fibrillation, the ventricular response is typically made of irregular RR intervals, i.e., mark beat-to-beat variation in ventricular cycle length. This irregular ventricular rhythm arises from AV nodal filtering of high fibrillation rate through concealed conduction. During atrial pacing, an early atrial impulse may propagate some distance in the AV node before being blocked. The block, which cannot be seen on the electrocardiogram, is therefore concealed. However, its occurrence can be detected by a prolongation of the conduction time at the next beat. Indirect evidence suggests that such a phenomenon occurs and repeat itself during atrial fibrillation.[20-23] However, the physiology of concealed conduction and its specific role during atrial fibrillation remain to be factually established. The present study assesses how concealed conduction alters

nodal function in normal AV node with a slow and fast pathway, and in fast pathway alone obtained after a slow pathway ablation.

CHAPTER I

CURRENT STATE OF KNOWLEDGE ON THE AV NODE

1. Definition of the AV node

Clinicians, anatomists, and physiologists presently use the term AV node with different meanings. The term AV node variably stands for the compact node alone,

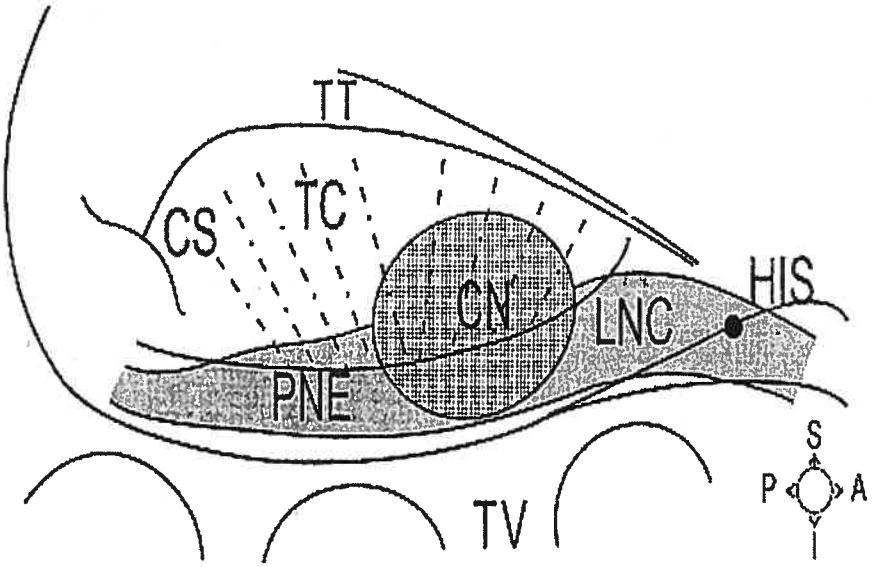

Figure I-1 Structures and landmarks of rabbit AV node. His, His bundle; LNC, lower nodal bundle; CN, compact node; PNE, posterior extension; TC, transitional cells; CS, coronary sinus; TT, tendon of Todaro; TV, tricuspid valve. From Medkour et coll.[15]

compact node and immediate surroundings, or entire atrial-His junction (Figure I-1). Tawara provided the first definition of the AV node that was then limited to the compact node.[1] Today, the specific role of the compact node in rate-dependent and dual pathway function remains unclear and very difficult to study. Meanwhile, it has become clear that

other structures, namely the transitional zone, posterior extension and lower bundle play critical role in nodal function. It has thus become necessary to redefine the AV node to take into account these developments. Thus, the AV node was recently redefined as including all structures (compact node, transitional zone, lower bundle and posterior extension) contributing to its recovery curve.[15,24] This definition was also adopted in a recent prestigious book.[25] In fact, a title search for AV node shows that most physiologists and clinicians adopted a similar broad definition of the AV node even though not explicitly expressed as such. In fact, of the numerous publications on the AV node, very few directly assess compact node function the role of which remains unclear.[26] The definition that includes all structures contributing to the nodal recovery curve is also used in the present study.[24,25]

2. Anatomy of the AV node

2.1 Location and structure

Working with Aschoff, Tawara[1] first demonstrated that the AV node connects the atrium to the His bundle. Subsequently, many studies[27-29] confirmed that the AV node lies in the lower posterior portion of the interatrial septum beneath the endocardium and an overlap of atrial tissue, anterior to the ostium of the coronary sinus, and directly above the insertion of the septal leaflet of the tricuspid valve (Figure I-2). Its landmarks were clearly described by Koch in 1909 within a triangle, which now bears his name, delineated by the membranous septum at its apex, the inferior border at the septal tricuspid leaflet, and the superior border at a strand of fibrous tissue extending from the central fibrous body to the sinus septum above the ostium of the coronary sinus (the tendon of Todaro).[28,30,31] The compact node is close to the apex of the triangle of Koch.

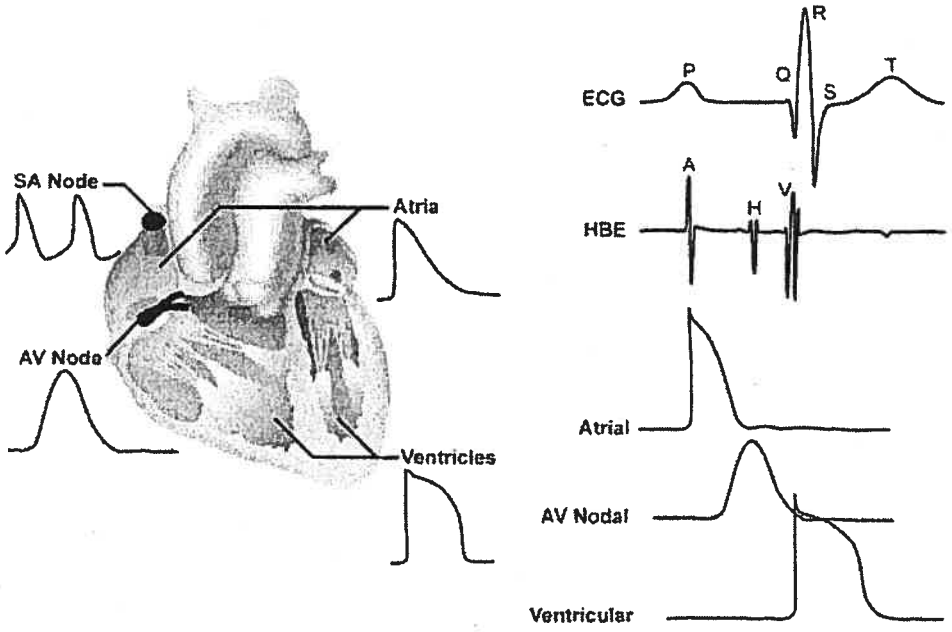

Figure 2. Relationship between action potentials and ECG. Left panel, typical action potentials from cells of various regions of the heart. Right panel, temporal correspondence between electrocardiogram (ECG), His bundle electrogram (HBE), and transmembrane action potentials recorded from atrial, AV nodal, and ventricular myocytes. From http://www.hrsonline.org/professional_education/learning_categories/articles/shrbel/Default.asp

The compact AV node varies in size in different species. In the rabbit, it is approximately 0.3 to 0.5 mm in length parallel to the septal insertion of the tricuspid valve, 0.8 to 1 mm in the depth in the direction from interatrial to interventricular septum, and 0.15 to 0.25 mm in thickness in the direction from right to left atrium.[32] In the adult, it measures approximately 5 to 7 mm in length and 2 to 5 mm in width.

The AV node of the rabbit heart has a complicated structure. Proximally, at the AV junctional region, the AV node has an extensive area in contact with the lower part of the

atrial septum. The transition from atrial fibers to transitional fibers occurs suddenly at the ultramicroscopic level.[33] However, this sudden transition does not occur at a detectable level macroscopically. Similarly, the connection between transitional cells and compact node cells remains poorly defined from a macroscopic point of view but the two types of cells have been shown to stain differently for connexins.[30] The compact node exhibits a complex interlacing of specialized myocardial cells. In the distal portion of the node, fibers align in a parallel fashion to form the penetrating portion of His bundle.[26,34] There are two main inputs to the AV node, an anterior and a posterior. The anterior input connects via the lower interatrial septum where the anterior and the middle internodal tracts descend and merge to form the superior margin of the AV node. The posterior input arrives at the node via the crista terminalis where the posterior internodal tract travels along right atrial endocardium and then into the interatrial septum above the coronary sinus, joining the posterior portion of the AV node.[26,34]

2.2 Action potential based functional zones

Based on electrophysiological characteristics (activation time and action potential configuration), Paes de Carvalho and de Almeida[35] divided the AV node into 3 zones: atrionodal (AN), nodal (N) and nodal-His (NH). The 3 functional zones form 3 layers that go from the His bundle to the coronary sinus ostium. However, there are no anatomic structures corresponding to the 3 layers. The N zones is confined to a small central area, surrounded at its anterior, superior and posterior margins by the AN zone while inferiorly making contact with the NH zone.[34,36] In the rabbit, the AN zone corresponds to a transitional cell group in the proximal portion of the node and is made of elongated small cells.[36,37] Moreover, a careful microelectrode-based mapping study conducted by Billette

showed that the AN cells in fact occupied a large area in the proximal portion of the AV node and can be subdivided into AN, ANCO (AN with component) and ANL (late AN) cells.[38]The NH zone corresponds to the lower nodal cell bundle that spreads from His bundle to coronary sinus. Initially considered as a dead-end pathway,[39,40] recent studies has considered the posterior portion going from the center of the node to the coronary sinus as corresponding to the posterior extension (Figure I-1).[15,41] The posterior extension is made of nodal-like cells. It connects anteriorly with the lower nodal bundle, which is made of elongated small cells near the connection and larger cells near the His bundle.

2.3 Blood supply and innervation of AV node

The AV node receives a disproportionately large arterial blood supply relatively to its small size. In most individuals, this blood supply comes from two main arteries.[42] One is the AV node artery, which arises at the crux of the heart and ascends to enter the AV junctional area. It is a branch of the right coronary artery. The second artery comes from the left anterior descending coronary artery as a septal branch.[43]

Numerous sympathetic and parasympathetic nerve branches richly innervate the AV node. The left and right cardiac sympathetic fibers, which come from the paravertebral chain of either the stellate ganglion, the ventral limb of the ansa subclavian, or the caudal cervical ganglion, project onto the posterior surface of the heart, then cross the superior pulmonary vein, sending branches to penetrate the AV groove and into the epicardium overlying the AV nodal region. Cardiac vagal ganglia supplying AV nodal region are found within a smaller fat pad overlying the epicardium at the junction of the inferior vena cava with left atrium, adjacent to the coronary sinus entrance. Recently, selective AV node vagal stimulation has emerged as a novel strategy to control ventricular rate

during atrial fibrillation.[44-48] When applied to the vagal ganglion, the stimulation achieves a desired average ventricular rate but unfortunately, the rate variability remains. More recently, Zhang et al[49] used this strategy combined with ventricular on-demand pacing to obtain a satisfactory ventricular rate and regular rhythm in mongrel dogs. This novel approach results in a regular, slow ventricular rhythm during atrial fibrillation that does not necessitate AV node ablation.

3. Basic electrophysiology of the AV node

3.1 Excitability

N and NH cells are hypoexcitable and recover slowly after activation.[9] their excitability is much lower than that of atrial and ventricular tissues. Microelectrode studies[35,50] revealed that N cells have a low resting membrane potential, low action potential amplitude, small or no overshoot, and slow rate of depolarization (low V_{max}) during phase 0. With intracellular stimulation and recording, Merideth et al[9] showed that the current requirement to reach threshold is higher in AV nodal area as compared to other cardiac tissues and that it is highest in N cells. They also demonstrated that the recovery of excitability lags beyond full repolarization in N cells. This delayed recovery increases with rate. This rate-dependent reduction in nodal cell excitability was demonstrated to be associated with a parallel depression of nodal conductivity.[9] A study by Hoshino et al[51] shows that, in single AV nodal myocytes, the recovery of excitability after an action potential follows a very slow time course and greatly outlasts the action potential duration. Such a slow recovery of excitability has been postulated to be responsible for the rate-dependent activation failure in these nodal myocytes.[51]

3.2 Refractoriness

An important characteristic of excitable cells is their refractory period which provides a limit to the maximal frequency of activation. Refractoriness can be

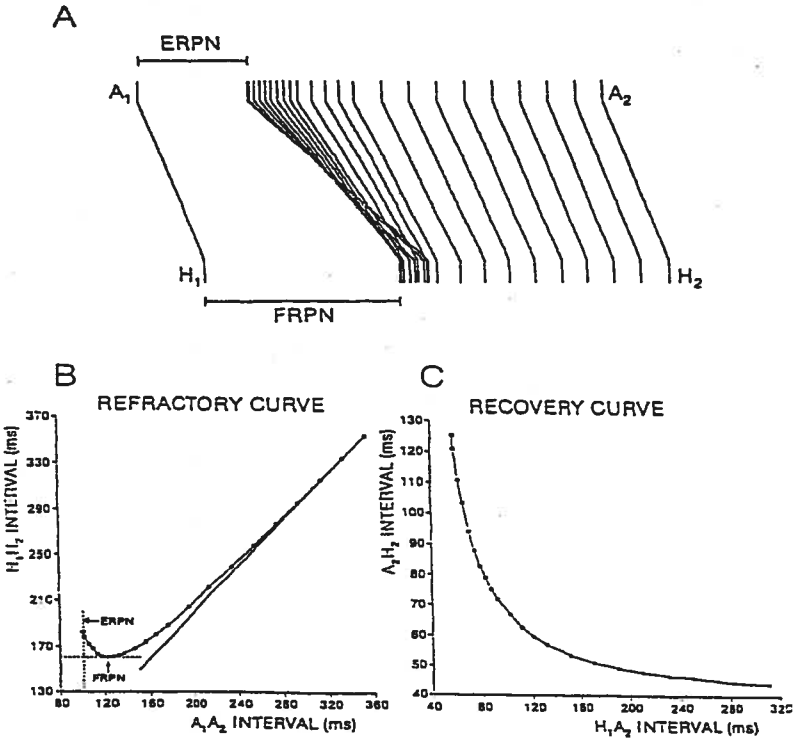

Figure 3 Methods used to characterize AV nodal conduction and refractoriness. A, superimposition, in reference to basic conduction time (A_1H_1), of premature conduction times (A_2H_2) obtained during a premature protocol in one rabbit heart preparation. B, refractory curve (H_1H_2 versus A_1A_2) with effective (ERPN) and functional (FRPN) refractory period. C, recovery curve obtained by plotting the A_2H_2 against corresponding H_1A_2. (Modified from Billette & Giles[2])

characterized at the whole AV node level with a premature protocol (a test premature impulse introduced with a variable coupling interval during a constant basic rate).

The resulting nodal responses are schematically superimposed in Figure I-3A and show that A_2H_2 increases with decreasing A_1A_2. These responses can be used to construct the nodal curve (Figure I-3C, A_2H_2 vs. H_1A_2 or A_1A_2) and obtain two indices of nodal refractoriness (Figure I-3B), which were first described by Krayer et al.[52] They are obtained by plotting the different inter-His (H_1H_2) intervals against the corresponding interatrial (A_1A_2) intervals.[6,14] The first index is the effective refractory period (ERPN), which is defined as the longest A_1A_2 interval that fails to generate a nodal response to A_2 (Figure I-3B). When an atrial block develops before nodal block, ERPN is approximated from the shortest A_1A_2 interval that results in a conducted A_2. The shortest H_1H_2 interval achieved yields the second index, called the functional refractory period (FRPN).

Both ERPN and FRPN have been clearly demonstrated to be rate dependent.[14,53,54] However, inconsistencies between the rate-dependent variations in FRPN and ERPN have been reported.[55-58] Cagin et al[59] demonstrated that an increase in heart rate prolongs ERPN but shortens FRPN. Conversely, Young et al[60] and Denes et al[56] showed a parallel change of FRPN and ERPN, in which both parameters decreased with the increase of heart rate. It was also observed that the FRPN and ERPN change in the same direction under the effect of epinephrine or atropine.[52,57,61,62] Moreover, differences in rate-dependent changes of ERPN between children and adults were also reported.[63] So far, there is still no consensus on whether FRPN or ERPN can best represent nodal refractoriness. Ferrier and Dresel[57] have reached the conclusion that there is a lack of relationship between FRPN and nodal refractoriness. Simson et al[58] also reported that FRPN can vary independently of changes in nodal refractoriness as measured by ERPN. Thus, they concluded that the FRPN is a complex parameter and does not reliably

measure refractoriness. However, Young et al[60] opposes the use of ERPN as an index of nodal refractoriness. Using Rosenblueth one-step delay hypothesis,[55] Young et al[60] assessed the effects of rate on nodal refractoriness and suggested that variations in ERPN come from changes in recovery time due to variations in basic nodal conduction time which in turn cause a phase shift of the recovery cycle rather than a real change in excitability. Thus, these authors considered that ERPN could not reflex real changes in nodal refractoriness unless it is corrected for the changes in basic nodal conduction time. After such correction, the rate-dependency of FRPN and the corrected ERPN were found to vary in the same direction.[14,60,64]

Billette and Métayer[14] studied the factors involved in the intrinsic regulation of the rate-dependent changes of FRPN in isolated rabbit heart preparation. These authors showed that, for a given fast rate, FRPN could vary markedly from beat-to-beat in a wide variety of patterns depending on the opposite effects of facilitation and fatigue. When present alone, facilitation and fatigue shortened and prolonged FRPN, respectively. Under combined effects of facilitation and fatigue, FRPN could be either shortened, unchanged, or prolonged depending on the state of interaction between these two properties.[14]

More recently, Tadros et al[65] studied AV nodal refractoriness with a protocol independently varying the effects of basic and pretest cycle, and reached the conclusion that FRPN consistently increases with fatigue and decreases with facilitation. ERPN also increases with fatigue and decreases with facilitation after correction for the changes in basic nodal conduction time. The changes in basic nodal conduction time are an important determinant of rate-induced changes in ERPN and may account for its

differences with FRPN. Fatigue, facilitation and changes in basic nodal conduction time effects account for nodal responses to standard protocols but cannot be easily exposed by standard protocols alone.[65]

3.3 Conductivity

As compared to other parts of specialized conducting system, the AV node has a low conductivity. Both anatomical and physiological factors contribute to this slow conduction. Two major anatomic factors are fiber diameter and geometric arrangement of fibers. Due to cable properties of fibers, the larger is the diameter of fibers, the easier and faster the impulses propagate. As to geometric arrangement of fibers, conduction velocity is greater when an impulse travels a fiber longitudinally than in a transverse direction.[66] Two major physiological factors are the effectiveness of stimuli originating from depolarized fiber and the excitability of responding fiber. An action potential with a greater amplitude and a faster rate of rise during phase 0 depolarization is a more effective stimulus and results in a greater conduction velocity than an action potential with a smaller amplitude and slow rate of rise.[67] The excitability cycle of responding fibers makes the time interval between two successive stimuli another important determinant of the impulse transmission.[9] If a depolarization wave arrives in a fiber prior to its full repolarization from a preceding excitation (i.e., in a partial refractory state), the recovery of excitability of this cell is incomplete and the resulting premature discharges provides less effective stimuli to the responding fibers.

3.3.1 Assessment of nodal conductivity with recovery curve

The changes of nodal conduction time with slow recovery of excitability can be characterized with a recovery curve (Figure I-3C). Such a curve is constructed from the

data obtained with a periodic premature stimulation. There are two approaches used to construct a recovery curve.[68] One consists in plotting the nodal conduction time of premature beats (A_2H_2 interval) against the corresponding recovery times (H_1A_2 interval).[2,10,68,69] The second approach differs from the first by the use of the A_1A_2 interval as the index of recovery times.[9,54,70,71]

Since the early twenties, the recovery curve has been widely used in describing the physiological or pathological characteristics of AV nodal conduction and in analyzing the changes produced by different atrial stimulation patterns and/or drugs. Mobitz[72] in 1924 used the recovery curve to analyze the PR-RP relationship and to characterize the Wenckebach periodicity. Lewis and Master also used the same approach one year later to study AV nodal function.[8] With the development of experimental intracardiac recording,[73-75] it became possible to dissociate the components of the PR interval in which the AH interval specifically represents the nodal conduction time. Henceforth, the recovery curve relating PR-RP or PR-PP intervals was recasted as relating AH interval versus HA or AA interval. The A_2H_2 vs. A_1A_2 curve provides the scheme from which nodal function is assessed in humans undergoing endocavitary investigations for cardiac arrhythmias.[76,77]

3.3.2 Location of the nodal conduction delay

Diverging opinions on the origin of conduction delay in the node have been expressed since the very beginning of this century. In 1913, Kure[78] suggested that the delay takes place in the upper part of the AV node while Zahn[79] assumed that the middle portion of the node is responsible for most of the conduction delay. Much later in 1958, Matsuda et al[80] achieved the first intracellular record from a nodal cell. Hoffman et al[50,75]

considered that the delay takes place at the atrial margin of the AV node. Paes de Carvalho and de Almeida who first proposed, based on their microelectrodes recordings from isolated rabbit heart, the AN, N and NH classification of AV nodal cells located the greatest slowing of propagation in the N zone.[35] However, changes of propagation velocity in AN zone are gradual and smooth until a minimum is reached in N zone. In the NH zone, the conduction gradually accelerated as the His bundle is approached. Billette provided more information about the sites of AV nodal delay.[38] This study demonstrated that the lowest upstroke velocities were found in N cells, which also had a greater prematurity-dependent increase in action potential duration. During premature atrial stimulation, action potential amplitude of N cell decreased, and the response dissociated into two components. According to this study, the AN and NH zone accounted each for 25% of the basic conduction delay whereas the central node (N to NH zone) accounted for close to 50% of the delay. This study also showed that the prematurity-dependent increase in nodal conduction time develops also mainly between the N and NH zones.[81]

3.3.3 Mechanisms of nodal delay

Hoffman and Cranefield[82] suggested that the nodal delay is due to decremental conduction. These authors considered that, as an impulse travels in nodal non-homogeneous tissues, it encounters tissues of progressively greater threshold, of decreasing space constant, of decreasing action potential amplitude, and of decreasing rate of depolarization, which combine to produce a progressive slowing of conduction. However, Rosenblueth[55] suggested that the conduction delay and its rate-dependent increase are due to a "one step delay" which occurs at one point in the conduction path rather than to overall decremental conduction. Several lines of evidence showing

discontinuous propagation in non-homogeneous tissues support this explanation.[69,83,84] Billette et al demonstrated that, with shortening of cycle length, action potential in the N zone dissociated progressively into two components that were synchronous with late AN and early NH activity, respectively.[37] No action potential upstrokes occurred during the interval between two components. The increase in nodal conduction time with shortening of cycle length was largely due to the "stagnation" between N and NH zone activation.[81] The stagnation is probably caused by cessation of active transmission at the unexcitable element, which can be nevertheless crossed by electrotonic current, bringing distal excitable cells to threshold as described in other cardiac tissues.[83,84] The ionic mechanisms of nodal conduction delay are not completely understood yet. It has been proposed that the slow recovery from inactivation of the slow inward calcium current and the slow deactivation of potassium current in the central AV node are important determinants of the nodal delay.[51,85]

4. Rate- and time-dependent properties of the AV node

4.1 Complexity and unpredictability of nodal behavior

An increase in heart rate usually induces an increase in nodal conduction time. However, the relationship between heart rate and nodal conduction time can vary in a very complex manner both with the rate itself and its duration. Disparate nodal conduction time may be obtained at identical heart rates reached with different approaches.[8,11-13] Nodal responses can also vary with the stimulation pattern used. For example, the addition of a single constant short cycle before the premature cycle result in a completely different set of premature nodal conduction time than those obtained without the additional short cycle.[11] Nodal response to an incremental pacing protocol

obtained by reducing the stimulus interval by 20ms at every 20th beat also have been shown to differ entirely from those induced by a similar incremental pacing but with 20 control basic beats being inserted between subsequent reductions.[12] The controls basic beats then prevents the occurrence of cumulative effects of rate. The initial condition from which a stimulation is started is also an important factor affecting the nodal behaviour.[13,86] Two identical periodic premature stimulations performed at the same fast rate, but one being started before and the other after reaching a steady-state nodal conduction time result in a very different nodal recovery responses.[81] Similarly, identical premature stimulation protocols performed at five different basic cycle lengths can result in five different nodal recovery curves.[81]

For a fixed heart rate, the nodal conduction time increases with the duration of the rate, an effect called fatigue.[8,12,13,57] The faster is the rate the greater is the fatigue developed. However, part of the increase in the nodal conduction time observed after a sudden increase in heart rate is not due to fatigue. Levy et al have demonstrated that there is then an inverse relationship between RP and PR interval.[7] However, the contribution of this factor is often ignored thus leading to overestimation of fatigue effects.[58] When a fast rate is imposed with a constant RP or HA interval, which prevents RP-PR or HA-AH variations, the fatigue can be directly obtained and is much less than in the absence of this control.[7,13] During transient responses such as those obtained during incremental pacing protocol recovery and fatigue effects occur together and cannot be easily dissociated.

To better understand the mechanism responsible for the complex nodal behavior, it is important to identify and characterize the underlying nodal functional properties

involved in the different steady-state and transient nodal responses. Lewis and Master[8] identified 3 different components in the rate-induced changes of the nodal conduction time: a conduction slowing of premature atrial impulses, an abbreviation of the nodal conduction time and refractory period caused by a single cycle of a faster rhythm introduced before the premature cycle, and an impairing cumulative effect of frequency on the nodal conduction time. In a series of studies, Billette et al[12-14,81] were able to dissociate and further characterize these 3 components which are now referred to as recovery time, facilitation and fatigue. Studiesalso indicate that the interactions between these 3 properties can account for a wide variety of nodal responses.[12,64,85,87-92]

4.2 Definition and characteristics of AV nodal functional properties

4.2.1 Recovery time

The recovery time represents the time elapsed since last activation and reflects recovery of excitability before next activation.[2] This time may be estimated by the His – atrial (HA) interval, which is the time from the beginning of a given His bundle activation to the beginning of the next atrial activation.[69] Recovery time is also frequently assessed by the atrial (AA) interval.[9,57,93] Because the node consists of many different cells which are activated in sequence (i.e., proximal nodal cells are activated and recover earlier than distal cells), there is no common recovery time for all nodal cells. When the preceding AA interval is used to assess nodal recovery time, the recovery time of distal nodal cells is overestimated when the nodal conduction time increases; the constant AA suggests that recovery time has not changed while in fact it has been shortened by the increased nodal conduction time. When the preceding HA interval is used to assess nodal

recovery time, the recovery time of proximal nodal cells is underestimated.[2,94,95] However, because the activation of proximal nodal cells is largely cycle length independent,[81] this bias may have a lesser impact than its overestimation with the AA interval.

Nodal recovery time is a major determinant of the variations of nodal conduction time in response to changed heart rate.[11,12,81,96] A shortened HA prolongs the next AH.[69] This effect increases more rapidly in the short HA range. At a shortened HA interval, the atrial impulse reaches the node earlier in the nodal refractory period. The shorter is the HA interval, the more refractory is the node, and the longer is the AH interval.[11,69] Nayebpour et al[87] characterized the effects of vagal stimulation on nodal recovery property. They showed that under vagal stimulation, nodal recovery was incomplete for a longer period after nodal activation, thus resulting in nodal block at longer recovery time, which could otherwise evoke a conducted beat.

Above studies suggest that the recovery time constitutes the major determinant of changes in nodal conduction time. However, the changes of recovery time alone cannot satisfactorily explain all rate-induced changes in nodal conduction time which are also contributed to by nodal facilitation and fatigue.[12,81]

4.2.2 Facilitation

Nodal facilitation is defined as a shorter nodal conduction time than expected from recovery time and fatigue.[11] It can be selectively characterized by simply adding a short cycle before the premature cycle during a protocol otherwise identical to that used for the determination of the recovery property. In addition, a conditioning intermediate cycle is also usually introduced before this short cycle to allow for an induction of the maximal

facilitatory effect. The intermediate cycle shortens the minimum facilitating cycle that can be tested. A facilitatory effect develops after one short cycle, remains constant during a lasting fast rate and dissipates after a single control long cycle.[11] Usually, one short cycle produces a maximum shortening in nodal conduction time and FRPN. Facilitatory effects are thus time-independent.[11,81] Graphically, facilitatory effect is manifested by a leftward shift and tilt of the HA-recovery curve in the short H_1A_2 range.

Nodal facilitation was first observed, though not named as such, by Lewis and Master in 1925.[8] However, its very existence remains debated. Several factors affect its manifestation. While facilitation is most easily seen on HA curve, it is also present and unchanged on AA curve but then hidden by greater effects of changes in basic nodal conduction time.[13,68] Its identification then requires the correction of AA curve for changes in basic nodal conduction time. Because not spontaneously seen on AA curve, several investigators tend to simply ignored facilitation.[71,94,95,97] However, careful examination of the published AA-recovery curves [9,57] does indicate the presence of facilitation which appeared as the convergence and/or crossing of the recovery curve in the short AA interval range. The facilitatory effects were studied by Billette et al[11,12,14,81] who successfully dissociated them from other rate-dependent effects. The presence of facilitatory effects has also been demonstrated during both transient and steady state nodal responses, and was found to occur concurrently with changes in recovery time and fatigue. In these circumstances, facilitation may be masked and difficult to identify. However, when changes in recovery time and fatigue are controlled or measures, it becomes possible to clearly identify the facilitatory effects.[12-14,85,88] Moreover, these studies indicate that the inclusion of facilitatory effects is a necessary condition to

quantitatively account for nodal conduction time observed in various rate-induced nodal responses.

4.2.3 Fatigue

Nodal fatigue is defined as the rate- and time-dependent prolongation of nodal conduction time occurring for comparable recovery time and facilitation level. The fatigue effect develops slowly during a fast rate and dissipate in a reverse symmetric pattern after the termination of the fast rate.[12,13,81] The slow time course of fatigue induction causes it to start affecting the nodal conduction time only several beats after the beginning of a fast rate and to take several minutes to reach a steady state. Similarly, the slow dissipation of fatigue may cause it to affect the nodal conduction time several minutes after the cessation of a fast rate.

Nodal fatigue has been reported by several investigators.[7-9,57] With sustained atrial pacing at a constant short cycle length, these authors observed cumulative increase of nodal conduction time which they called "exhaustion" or "fatigue". However, these authors did not dissociate per se from the effects of uncontrolled changes in recovery time which accounted for an important fraction of the nodal conduction time prolongation that they observed. In later studies, Billette et al[12-14,81] selectively characterized nodal fatigue and distinguished it from other recovery-dependent effects. These induction and dissipation of fatigue were shown to follow an almost symmetric slow time course.[13] During periodic premature stimulation performed at a constant fast basic rate but no pre-established steady state, fatigue grew progressively with the duration of the rate needed to test the different premature beats.[81] Therefore, despite the same rate, the two approaches

then resulted in different nodal responses. Both the rate itself and its duration are important determinants of the level of fatigue reached.

5. Dual AV nodal pathways

Dual AV nodal pathway electrophysiology has long been accepted as the basis for AV nodal reentrant tachycardia (AVNRT).[98-103] The outstanding success of ablation therapy for AVNRT over last two decades has further focused the attention of cardiac electrophysiologists on this topic.[5,104-106] The basic underlying concept is that the AV node can be functionally split into two pathways (a slow and a fast) with different conduction and refractory properties that favor the initiation of reentry.[99] The fast pathway conducts rapidly and is thereby dominant but has a long refractory period. When the coupling interval reaches a value shorter than the refractory period of the fast pathway, the slow pathway can, due to its short refractory period, take over conduction. The transition from fast to slow conduction is frequently associated to a sudden increase in A_2H_2 and the initiation of echo beats in patients suffering from AVNRT. There is a general agreement that the slow pathway originates somewhere in the posterior portion of the node and is connected to the crista terminalis input while the fast pathway is located more anteriorly and connected to the interatrial septum. This is also supported by the fact that ablation therapy targeted at the posterior input interrupts the slow pathway while an ablation at the interatrial septum interrupts the fast pathway.[4,107,108] However, the exact anatomic and functional substrate underlying the dual pathways remains debated.

Mendez and Moe initially proposed that the two pathways reflect a functional asymmetry between the crista terminalis and interatrial septum inputs with their prolongation to some undefined distance into the compact node.[99] The remaining distal

portion of the node would form a common distal pathway. The fact that input-targeted ablation therapy does not involve compact node legions indicates that the compact node may not be an important determinant of dual pathways, leaving the inputs as the primary substrate. There is evidence of some degree of functional asymmetry between the two inputs.[101,103,109-114] Several investigators have recorded double component action potentials in the input areas and some have attributed it to dual pathway physiology. However, this question was thoroughly reassessed recently by de Bakker et al[115] who concluded that that double potentials are unlikely due to dual pathway physiology.

In an effort to formerly establish the role of functional asymmetry between the inputs in dual pathways, Amellal et al[116] characterized them with local stimulation and recording techniques. They found that the two nodal inputs have equivalent conduction and refractory properties, and are equally effective in activating the rate-dependent portion of the node. Their findings predict that, even for symmetric functional properties of the inputs, an impulse entering the node from the low septum could be blocked at the anterior nodal input but propagated from the posterior input, thus resulting in an nodal conduction time prolongation when measured from His bundle lead. This prolongation is due to the extra traveling time of the impulse toward and in the low crista input rather than actual changes in input conduction velocity. Their results suggest that the proximal node acts as a matching gate that enables widely varying atrial wave fronts into equally effective activation signals for the rate-dependent portion of the node.

The search for alternative substrate led to the development of a new model in which the slow and fast pathway would be provided by the posterior extension and compact node, respectively.[15-19] In this model, the two inputs form a common proximal pathway

while the lower bundle forms a common distal pathway. Although the characteristics of the demonstrated dual pathways differed from those of AVNRT patients, the dual pathways were found in all rabbit hearts studied, thus establishing that dual pathways is a normal feature of rabbit AV node. The posterior extension is also consistently present in humans but its functional role remains to be established.[41] Recent dye mapping studies have provided further direct evidence for this model by demonstrating that it is compatible with the characteristics of local activation during echo beats.[25,117-119]

The discontinuous AV nodal conduction curve has been used clinically as evidence for the existence of dual AV nodal pathways. The criterion used to identify such a discontinuity is the occurrence of a 50-msec jump in AH for a 10-msec decrement of the atrial coupling interval during delivery of programmed premature atrial beats.[120] The two portions of the discontinuous conduction curve are thought to represent a shift of the conduction from fast to slow pathway when the long effective refractory period of the fast pathway has been reached. While many AVNRT patients show such a discontinuity, not all patients do. Moreover, some patients without AVNRT do have a jump in AH intervals. Thus, the link between the jump in AH and AVNRT is a frequent but not a necessary one. In order to explain this phenomenon and the presence of residual AV nodal conduction after ablations of slow and fast pathways, Hirao et al[111] suggested the existence of intermediate pathway(s). Anterograde conduction over the intermediate pathway would smooth the transition from the fast pathway to the slow pathway, resulting in a more continuous curve. Similarly, anterograde conduction over the slow pathway without retrograde exit can cause a discontinuous curve with no inducible AVNRT. Recently, several investigators have shown that dual AV nodal physiology can

be deduced in patients without discontinuous AV nodal conduction curves by the following findings after radiofrequency ablation in the region of the slow pathway: (1) an increase in the anterograde AV nodal effective refractory period; (2) an increase in the anterograde Wenckebach cycle length; (3) shortening of the maximum AH in response to atrial extrastimuli and, (4) loss of the tail of the smooth AV nodal conduction curve.[121,122]

Recent mapping and ablation studies support several postulates. 1) The fast and slow pathway represent different atrionodal connections rather than a result of longitudinal dissociation within the compact node.[5,107,111] 2) These pathways are functional pathways instead of cable-like structures.[123] 3) Multiple AV nodal input pathways likely exist as suggested by the presence of residual AV nodal conduction after ablations of fast and slow pathways.[111]

6. Concealed conduction

In 1894, Engelmann[124] stated that every effective stimulus applied to the atrium, even if it is not followed by a ventricular response, lengthens the next AV interval. The mechanism underlying this effect was investigated much later. In 1925, Ashman[125] studied the influence of blocked impulses on subsequent conduction in compressed atrial muscle of the turtle heart. He observed that the earlier the blocked impulse follows a transmitted one, the less is its effect upon the conduction time of a subsequent transmitted impulse. Conversely, the later is the blocked impulse after the transmitted one, the greater is its effect upon subsequent conduction. Levis and Master[8] in their classical observation upon AV conduction in the mammalian heart demonstrated clearly that, in 2:1 AV block, whether produced by raising the atrial rate, or by stimulating the vagus, the conduction intervals are lengthened by the presence of the alternate atrial beats, that is, those to

which the ventricle fails to respond. In 1948, the term concealed conduction was first introduced by Langendorf[126] and used to describe such a phenomenon by which an atrial impulse activates a portion of the AV node before being blocked. This phenomenon is now considered a major determinant of nodal responses during supraventricular tachyarrhythmias.[21,127-129] In 1965, Langendorf et al[128] demonstrated successfully the existence of concealed AV conduction and its influence on subsequent conduction in the human heart. The prolongation of the P-R interval after interpolated ventricular premature systoles is the most obvious example of this phenomenon. The retrograde impulse of the ventricular premature systole penetrates into the AV node and is stopped before reaching the atrium; this results in a prolonged A-V conduction time at the postextrasystolic beat. Even if this partial penetration does not result in any specific electrocardiographic wave, its effect can be detected from the influence it has on the AV nodal conduction or PR interval at the next beat.

Although the supporting evidence is so far very limited, concealed conduction is considered to play a major role in the gross irregularity of ventricular response to atrial fibrillation. At the same time, summation and cancellation of atrial impulses entering the AV node at different inputs, rates and degrees of regularity as well as autonomic tone may all contribute to the high irregularity of ventricular response to atrial fibrillation. However, their sorting out may require that the mechanisms underlying concealed conduction be first better understood. Another difficulty in attributing the gross irregularity of the ventricular response to concealed conduction is its puzzling link with the refractory period. If, as now generally accepted, the ventricular response to any type of rapid atrial activity is primarily determined by the refractory period of the AV

junction, one would expect a more regular response of the ventricle than observed during fibrillation. Indeed, because an atrial impulse is always immediately available to the node at the termination of its refractory period, RR intervals should have values approximating this refractory period, which is obviously not the case. The duration of the refractory period could be altered and the regularity of the ventricular rate disturbed, if one or more of the atrial impulses penetrate into the AV junction without reaching the ventricles. Such concealed conduction of any impulses will affect conduction of the subsequent impulse by delaying it, blocking it entirely, or causing repetitive concealed conduction.[20,130] Concealed propagation of the atrial impulse may occur during various portions of the heart cycle and reach different levels within the AV junction. The varying depth of nodal penetration and its varying time of occurrence is likely to result in much variation in cell refractoriness. These different effects at different AV junctional levels will favor secondary concealment and repetition of long ventricular cycles. The above possibilities proposed by Langendorf[130] in 1965 were further supported by later studies. Benefiting from technical progresses and a better understanding of anatomy, electrophysiology, and functional properties of AV node, several physiologists have used again these basic concepts that have become guiding principles in the study of concealed conduction. Whatsoever, current evidence indicates that the block is due to both increasing refractory period and decreasing excitability in temporally more distal portions of the AV node. These properties cause a premature test impulse to be blocked increasingly more proximally when introduced with decreasing coupling interval.[9,34,38] Potential sites of block are numerous but the junction between transitional and compact node tissue

constitutes a critical prevalent one.[127] Whether the blocked beat affects only the activated portion of the AV node or also the distal inactivated part remains unclear.

There is evidence that a concealed beat postpones the recovery of nodal excitability as reflected on nodal curve (A_2H_2 vs. A_1A_2).[97,131] The blocked beat would prolong refractoriness and postpone the recovery cycle in cardiac cycle. Recently, a study by Liu et al[132] stated that the concealed beat prolongs refractoriness of proximal cells and prevents assessment of real refractoriness in more distal nodal elements that may or not have changed. They also proposed new data and concept suggesting that events occurring in slow pathway may play a critical role in concealed conduction. They showed that a concealed beat amputated the left portion of AV node curve (manifest portion of slow pathway) in both AVNRT and control non-AVNRT patients. The concealed beat prolongs ERPN and reduces A_2H_{2max} in both groups. In AVNRT patients, the concealed beat reduces the incidence of discontinuous curve and AVNRT induced by premature stimulation. In other words, the concealed beat prevented slow pathway conduction in a similar manner than did slow pathway ablation. Moreover, the concealment effects on fast pathway conduction were similar before vs. after slow pathway ablation. Thus, the understanding of AV nodal concealed conduction may require the sorting out of different individual effects induced in fast and slow pathway.

The finding that a concealed beat prevents manifest slow pathway conduction but shifts the fast pathway curve to the right is an intriguing one.[132] The primary riddle is whether the concealed beat reduces excitability and prolongs refractoriness in slow pathway. A primary objective of the present study was to assess the role of slow pathway in concealed AV nodal conduction.

7. AV nodal function during atrial fibrillation

Concealed conduction is assumed to play a key role in the gross irregularity of the ventricular response to atrial fibrillation.[20,82,133,134] Because it can repeatedly occur, concealed conduction would generate different ventricular cycle lengths during atrial fibrillation. The cycle length would then vary with the number of concealed beats. Shortest RR intervals would be imposed by FRPN and would occur when there is no concealed beat.[135] Longer RR intervals would depend on the number of concealed beats.[82,136] Three mechanisms have been proposed to explain concealed conduction during atrial fibrillation: (1) decremental conduction,[35,137] (2) electrotonic modulation of automaticity[138] and, (3) electrotonic modulation of propagation.[83,139]

The idea of decremental conduction comes from the original studies of Hoffman et al[137] who proposed that the AV node was the site for slow but continuous conduction of electrical impulses from atrium to the His bundle. As the impulses travel across the center of the node, a progressively increasing threshold, a decreasing space constant, and a decreasing amplitude and rate of rise of the action potentials would lead to a gradual decay of the effectiveness of the active regions to depolarize more distal tissues. Accordingly, block can occur if the area of decremental conduction is sufficiently long. It is important to note that decremental conduction can only occur in homogeneous and continuous excitable media. This is clearly not the case for the AV conducting system, which is highly heterogeneous and discontinuous.[140] Other studies[141-143] have concluded that it is difficult to explain the complex activity of AV node during atrial fibrillation in terms of decremental conduction.

The pacemaker properties of the AV node are manifest during AV block or atrial arrest. This phenomenon arises from the intrinsic automaticity of the AV node and its potential pacemaker role. This was recognized by Lewis in 1925 on the basis of the similarity in structure with the sinus node.[144] The frequency of such an oscillator can be modulated by external periodic electrical phenomena.[145] Cohen et al[146] later developed a theoretical model of an AV nodal pacemaker during atrial fibrillation. The model can explain several mathematical characteristics of the ventricular rhythm during atrial fibrillation. Amongst others, it accurately predicts the effects of right ventricular pacing or of a ventricular extrasystole during atrial fibrillation. However, the AV node as a pacemaker cannot explain the absence of scaling of atrial rhythm during atrial fibrillation.[147] Also, an AV nodal pacemaker might be suppressed by the overdrive caused by the rapidly incoming atrial impulses. Thus, electrotonic modulation of AV nodal automaticity is unlikely responsible for random rhythm during atrial fibrillation.

Electrotonic modulation of AV nodal propagation may account for some characteristics of the ventricular response during atrial fibrillation. When an impulse initiated in the atria or ventricles is blocked in the AV node, the blocked depolarization is obviously subthreshold for cells distal to the site of block. This subthreshold event is associated to electrotonic current flowing from depolarized to nondepolarized cells. Such distal effect of blocked beat ahead of the site of block can be demonstrated using microelectrode recordings of AV node action potentials during premature stimuli.[99] It has been shown that electrotonic depolarization can have profound effects on the electrophysiologic properties of the tissue distal to the block.[139,148] Antzelevitch and Moe[149] used two different models of isolated cardiac Purkinje fibers to demonstrate that

electrotonic depolarization can produce delay or even blockade in the transmission of subsequent impulses, depending on their timing. They used the term electrotonic inhibition to describe this phenomenon and suggested that many published clinical examples of concealed conduction may be explained in terms of electrotonic inhibition of excitability. More recently, Davidenko et al.[150] demonstrated electrotonic inhibition of excitability in single ventricular myocytes under current clamp conditions. Liu et al[151] studied the ionic mechanisms of electrotonic inhibition and determined the cellular basis of concealed AV nodal conduction. Results demonstrated that electrotonic inhibition was the result of partial inactivation of the transient calcium current ($I_{Ca,T}$). In addition, Liu et al[151] demonstrated that the ability of the subthreshold response to prevent subsequent excitation of an AV nodal cell was increased when the interval between the conditioning subthreshold pulse and the succeeding pulse was shortened, or when the amplitude of the subthreshold pulse was increased. Moreover, when a premature impulse fails to traverse the AV node, the subthreshold depolarization elicited downstream of the site of block led to a transient reduction of excitability, with consequent delay or block of the following impulse. Such results have provided the strongest evidence to date in support of the idea that at least some of the manifestations of concealed AV nodal conduction can be the result of electrotonic inhibition secondary to a transient decrease in $I_{Ca,T}$. The exact role of such mechanism during beat-to-beat changes in RR intervals remains to be established.

OBJECTIVES

The specific objectives of this project are as follows:

1) Characterize the concealment zone and concealed conduction effects in intact node (slow and fast pathway conduction) and after a slow pathway ablation (fast pathway conduction).
2) Develop a model based upon the use of a conditioning cycle introduced before the concealed cycle to induce a broad consistent concealment zone.
3) Study the effects of the conditioning cycle on the concealment zone and concealed conduction effects in intact node (slow and fast pathway conduction) and after a slow pathway ablation (fast pathway conduction).
4) Determine the effects of the concealed cycle length concealed conduction effects .
5) Develop a functional model of concealed conduction that accounts for concealment properties of both intact node and fast pathway.
6) Apply this new knowledge to the understanding of ventricular response to atrial fibrillation.

CHAPTER II

MANUSCRIPT IN PRESS IN HEART RHYTHM

CONCEALED CONDUCTION IN NODAL DUAL PATHWAYS: DEPRESSED CONDUCTION, PROLONGED REFRACTORINESS OR RESET EXCITABILITY CYCLE?

Short title: Concealed Conduction and Dual Pathways

Bochun XU, Jacques BILLETTE and Michel LAVALLÉE

Département de physiologie, Faculté de médecine,

Université de Montréal, Montréal, Canada

Supported by Canadian Institutes of Health Research, and

Heart and Stroke Foundation of Quebec

Address for correspondence:
Dr Jacques Billette
Pavillon Desmarais # 2135
Départ. Physiologie (Fac. Médecine)
Université de Montréal
CP 6128, Succ CV
Montréal (Québec)
Canada, H3C3J7

Tel : 514-343-7953
Fax : 514-343-2111
E-mail: [redacted]

ABSTRACT

Background: Concealed conduction is recognized as a major determinant of atrioventricular (AV) nodal filtering properties but little is known about the underlying mechanisms.

Objective: To consistently elicit concealed conduction through AV node and determine the involvement of slow and fast pathway in resulting changes in nodal function.

Methods: The concealment zone (ERPN minus FRP of atrium) was determined in 6 rabbit heart preparations with and without a conditioning cycle (10 ms longer than ERPN). Nodal function curves were constructed for concealed cycle lengths selected within the concealment zone. Experiments were repeated after slow pathway ablation.

Results: When assessed with a blocked beat alone, a narrow concealment zone (22±12 ms, n=3) was observed in 50 % of the preparations. In contrast, when assessed with a blocked beat preceded by a conducted conditioning beat, a wider concealment zone (77±47 ms, n=6, $p<0.03$) was observed in all preparations. Increases in the concealed cycle length resulted in graded increases in ERPN and FRPN, and graded rightward shifts of the recovery curve as a whole, consistent with a resetting of the excitability cycle in slow and fast pathway. These effects were analogous to those expected from a conducted beat. Slow pathway ablation widened the concealment zone but failed to alter fast pathway resetting.

Conclusions: Our approach reveals a wide concealment zone consistently displayed in all preparations. Concealed conduction acts as a resetting mechanism of slow and fast pathway excitability cycle similar to that expected from a conducted beat.

Keywords: Slow pathway, fast pathway, conduction, refractoriness, electrotonic modulation

List of Abbreviations:

ERPN, nodal effective refractory period

FRPN, nodal functional refractory period

P, protocol

AV, atrioventricular

A_1, basic atrial beat

A_2, test atrial beat

A_0, concealed atrial beat

A_1', conditioning atrial beat

INTRODUCTION

The AV node exhibits concealed conduction and dual pathway properties. Concealed conduction refers to a partial activation of the AV node that fails to reach the His bundle.[1-7] This leads to increases in conduction time and refractory period of the next beat, which presumably account for nodal filtering during supraventricular tachyarrhythmias. Repeated concealments and varying depth of nodal penetration of concealed beats may both contribute to irregular RR intervals in atrial fibrillation.[8-11] However, attempts to predict RR intervals during atrial fibrillation using concealed conduction indexes have yielded inconsistent results.[12,13] The poor predictive value of these indexes may reflect our limited knowledge of concealed conduction properties of slow and fast pathway.[14-17] A better understanding of these properties may help explain why the slow and fast pathway can both conduct and block impulses during atrial fibrillation,[18,19] yet only slow pathway ablation reduces mean ventricular rate.[20-22] In that connection, a concealed beat may impair slow pathway conduction in patients in a way similar to ablation.[15,16] The aim of the present study is to determine the role of slow and fast pathway in concealed conduction effects. To this end, we have developed a stimulation approach that consistently reveals a wide concealment zone. This allowed us to more completely assess the effects of increasing concealed cycle lengths over the concealment zone before and after a slow pathway ablation. Our data suggest that a resetting of excitability cycle in slow and fast pathway may be the basis for concealed conduction.

METHODS

Preparation, Apparatus, and Ablation

Experiments were performed in 6 superfused isolated rabbit heart preparations. Animal care was according to guiding principles of the Declaration of Helsinki. The preparation, perfusion system, Tyrode solution, stimulation techniques, and recording

system have been previously described.[23-25] The isolated tissue studied included the right atrium, AV node area, and upper right ventricle (Figure 1A). A bipolar platinum-iridium stimulation electrode was placed on the upper atrium. Unipolar electrograms were recorded from the upper atrium, crista terminalis, interatrial septum, posterior extension and His bundle with 250-μm insulated silver wire. The reference electrode was placed in Tyrode solution. Slow pathway ablation was performed with 3±1 microlesions targeting the posterior extension (Figure 1A). Slow pathway ablation was confirmed by the selective loss of the steep rising portion of the nodal recovery curve.[24,25]

Protocols

Ladder diagrams of atrial and His bundle beat sequences resulting from the 4 stimulation protocols are schematically illustrated in Figure 1B. The 4 protocols were performed before and after slow pathway ablation at a constant basic cycle length (15 A_1A_1 intervals, 30-ms shorter than spontaneous sinus rhythm. Stimulation intervals (250-μs resolution) were generated with a computer algorithm. All stimuli were twice threshold 2-ms pulses applied to the upper atrium.

Four premature stimulation protocols were used (Figure 1B). In protocol P1, a premature stimulation is periodically introduced with a decreasing coupling A_1A_2 interval as commonly performed. This allowed to establish control nodal properties. The concealment zone was scanned in 5-ms steps until an atrial block occurred. The upper limit (ERPN) and lower limit (shortest A_1A_2) of the concealment zone[4,16] were then determined at 1-ms precision. In protocol P2, a concealed A_0 beat was introduced between A_1 and A_2. The 0 subscript refers to the concealed beat, not conducted to the His bundle. The A_1, A_0, A_2 notation was adopted from a recent human study on the effects of concealed conduction on dual pathways.[16] The concealed cycle (A_1A_0) was varied as described further below. Protocol P3 was designed to assess the effects of a conditioning cycle (10 ms longer than control ERPN) on nodal function curves and concealment zone (Figure 1B). $A_{1'}$ refers to the conditioning atrial beat. The concealment zone was then

established by decreasing $A_1 \cdot A_2$ as described under P1. In protocol P4, the combined effects of the conditioning beat ($A_1 \cdot$) and concealed beat (A_0) on nodal function curves were determined. P4 differs from P2 by the conditioning cycle.

The concealed cycle lengths tested with P2 and P4 were selected from the concealment zone established under P1 and P3, respectively. The range of the concealed cycle lengths studied corresponds to the concealment zone less 5 ms from upper and lower limits. Five equally distributed concealed cycle lengths differing by at least 10 ms were selected. For short concealment zones, the number of concealed cycles was reduced accordingly but the 10-ms minimum difference was maintained. Any concealed cycle inducing atrial reentry was discarded. In all protocols, the coupling interval of the test beat (A_2) was decremented in 20, 10, 5, and 1 ms steps as cycle length decreased. A_0A_2 and $A_1 \cdot A_2$ intervals were tested over a range that exceeded A_1A_2 baseline value by up to 150 ms. This allowed the lower portion of the nodal recovery curve to be explored even when a conditioning and/or concealed cycle caused a rightward shift of the curve. Stability was verified by ensuring that A_2H_2min (minimum nodal conduction time) remains constant throughout the different protocols. A_2H_2min did not vary significantly with the concealed cycle length nor was it affected by the conditioning cycle and/or slow pathway ablation.

Interval Measurements

Electrograms (bandwidth 0.1 Hz to 3kHz) were digitized on-line at 5 kHz per channel. Signals were treated with the Axoscope program (Axon Instruments, Foster City, CA, USA) and analyzed off-line with the DATAPAC 2000 program (Run Technologies, Mission Viejo, CA, USA). Nodal conduction time was determined from crista terminalis and interatrial septum signal to His bundle signal. Because conduction times did not differ between these two inputs, only crista terminalis data are being presented. Nodal responses to P1 were depicted as a nodal recovery curve (A_2H_2 vs. A_1A_2, conduction time of test beat vs. preceding atrial cycle length) and refractory curve

(H_1H_2 vs. A_1A_2, test His bundle cycle length vs. corresponding atrial cycle length). From these curves, A_2H_2min, A_2H_2max, ERPN and FRPN were determined. In P2, P3, and P4, the atrial cycle length was measured by $A_1A_0A_2$, $A_1A_1'A_2$and $A_1'A_0A_2$, respectively. Recovery curves were also constructed using A_0A_2 or $A_1'A_2$ to assess the atrial cycle length before the test beat.[4-6,15] ERPN was the longest A_1A_2, $A_1A_0A_2$, $A_1'A_2$ or $A_1'A_0A_2$ not conducted to His bundle. FRPN was the shortest H_1H_2 or $H_1'H_2$ reached. In the current study, we have considered that the AV node includes all structures contributing to the recovery curve i.e., compact node, transitional cells, posterior extension and lower bundle.[26,27] Data were analyzed with multifactorial analyses of variance and paired t-tests using SPSS-11 for Windows (SPSS, Inc., Chicago, IL, USA). Results are reported as mean ± SD.

RESULTS

Concealment Zone: Effects of Stimulation Sequence and Slow Pathway Ablation

When assessed with a blocked beat alone (P1), a narrow concealment zone (22±12 ms, n=3) was present in 50 % of the preparations (Figure 2). When the blocked beat was preceded by a conducted conditioning beat (P3), a markedly increased concealment zone (77±47 ms, n=6, $p<0.03$) was observed in all preparations. Slow pathway ablation increased the concealment zone when assessed with a blocked beat alone (45±14 ms, n=6, $p<0.03$, closed circles in Figure 2). With a conducted conditioning beat, the concealment zone was further increased after ablation and its variability was reduced (67±6 ms, n=6, $p<0.02$, open circles). However, the combined effects of ablation and a conditioning cycle did not differ significantly from those obtained with a conditioning cycle alone before ablation. This may be related to the longer conditioning cycle after ablation (108±12 ms vs. 133±14 ms, $p<0.01$). While the upper limit of the concealment zone was increased by the conditioning cycle and ablation, the lower limit was maintained (Table 1). Interestingly enough, a conditioning cycle and/or ablation revealed a wide concealment zone in the 3 preparations lacking one under P1. In the aggregate, a

conditioning cycle or slow pathway ablation consistently revealed a wide concealment zone, not apparent when assessed with a blocked beat alone.

Effects of Concealed Cycle Length, Conditioning Cycle and Slow Pathway Ablation on Nodal Recovery Curve

With a blocked beat alone, the effects of concealed conduction on the nodal recovery curve could only be studied in the 3 preparations showing a narrow concealment zone. In contrast, a wide range of concealed cycle lengths could be studied in all 6 preparations when the concealed cycle followed a conditioning cycle. The primary effect of a concealed beat was to produce a graded rightward shift of the entire recovery curve that increased with concealed cycle length. This rightward shift was displayed with and without a conditioning cycle as well as before and after slow pathway ablation.

The effects of concealed cycles tested with P2 and P4 on nodal recovery curves are illustrated in Figures 3 and 4. In Figure 3A, concealed cycles tested under P2 caused a typical rightward shift of the nodal recovery curve. Because of the 10-fold wider concealment zone after a conditioning cycle, longer concealed cycles could be tested under P4 (Figure 4A). Nodal recovery curves underwent a proportionately greater rightward shift than under P2. All rightward shifts of the recovery curves were associated with trivial changes in shape and A_2H_2max (maximum conduction time). Under P1, mean A_2H_2max was 172±17 ms. Under P4, A_2H_2max slightly decreased to 145±34 ms and 141±26 ms at minimum and at maximum concealed cycle length but statistical significance was not reached. A_2H_2max did not correlate with concealed cycle length ($r=0.17$, NS).

The effects of slow pathway ablation on nodal responses to concealed beats tested under P2 and P4 are shown in Figures 3B and 4B, respectively. The most striking effect of ablation was the shortening of A_2H_2max in all recovery curves, as expected from previous studies.[24,25] Ablation significantly ($p<0.01$) reduced A_2H_2max to 120±15 ms under P1, and to 116±15 ms and 131±8 ms at minimum and maximum concealed cycle

length, respectively. As concealed cycle lengthened, A_2H_2max slightly increased from its post ablation value ($r=0.62$, $p<0.01$). Under P2, ablation caused greater rightward shifts of the recovery curve (Figure 3B vs. 3A) because longer concealed cycles could be tested in a wider concealment zone. Under P4, the concealed cycle range was reduced because of a longer conditioning cycle. Consequently, the rightward shift of the recovery curves was reduced (Figure 4B vs. 4A).

From the above observations, it is apparent that interventions increasing the concealed cycle length proportionately augment the rightward shift of the recovery curve without altering its shape. This dependence on concealed cycle length was maintained after slow pathway ablation.

Effects of Concealed Cycle Length, Conditioning Cycle, and Slow Pathway Ablation on Nodal Refractory Curve

The primary effect of a concealed beat is to curtail the left portion of the refractory curve and thereby prolong both ERPN and FRPN (Figure 5). Figure 5A shows nodal refractory curves obtained before slow pathway ablation in one preparation. With a blocked beat alone (P2), the left portion of the refractory curve was abbreviated with respect to control. ERPN and FRPN increased accordingly. In contrast, the right portion of the curve was not altered and remained on the identity line. The effect of a conditioning cycle alone (P3) was to bodily displace the curve to the right, thereby altering the reference from which concealed conduction effects occurred (Figure 5A). When tested with a conditioning cycle (P4), the concealed beat curtailed the left portion of the refractory curve at long but not at short concealed cycle lengths. Therefore, prolongations of ERPN and FRPN became more apparent as concealed cycles lengthened.

The effect of slow pathway ablation alone was to abbreviate the left steep rising portion of the refractory curve with respect to control (Figure 5, B vs. A). This led to increases of ERPN but not of FRPN. Concealed beats with and without conditioning

cycles curtailed the left portion of the refractory curves, and prolonged ERPN and FRPN, as concealed cycles lengthened. However, the conditioning cycle alone caused a rightward shift of the refractory curve from which concealed beat effects were referenced (Figure 5B). When compared to before ablation, the extent of the rightward shift of the refractory curves caused by the conditioning cycle was smaller.

Table 2 summarizes mean ERPN and FRPN values under P1, P3, and P4 before and after slow pathway ablation. Because P2 could be tested in only 3 preparations before ablation, data were not reported therein nor included in statistical analyses. The conditioning cycle alone (P3) significantly prolonged ERPN and shortened FRPN as compared to P1 both before and after slow pathway ablation. As the concealed cycle lengthened (P4), both ERPN and FRPN significantly increased when compared to P1 or P3. Except for an increase in ERPN under P1, ablation had no statistically significant effects on ERPN and FRPN.

As illustrated in Figure 6A, ERPN values linearly increased with concealed cycle length. Data points obtained before and after slow pathway ablation closely overlap. Two factors contributed to this increase in ERPN. The conditioning cycle alone increased ERPN by shifting the refractory curve to the right (Figure 5) over which concealed conduction effects developed. When examined for the 6 preparations, this rightward shift was proportionate to the nodal conduction time (A_1·H_1·) of the conditioning beat (Figure 6B). Values obtained after slow pathway ablation occurred over a shorter A_1·H_1· range because of longer conditioning cycles but the linear relationship overlapped data obtained before ablation (Figure 6B). Data point clusters indicate little variations of the rightward shifts in the face of different concealed cycle lengths provided that the conditioning cycle remains the same. The second factor involved in ERPN prolongation was the concealed cycle length itself (A_1·A_0). When ERPN is measured from A_1·A_0A_2, it unavoidably includes A_1·A_0, which is protocol-defined. Consequently, an increase in A_1·A_0 is bound to increase ERPN accordingly (Figure 6C). Conceivably, the concealed cycle length may

also affect ERPN by altering the corresponding A_0A_2. Figure 6D shows trivial changes in A_0A_2 at ERPN with concealed cycle length.

As for ERPN, a close relationship was found between FRPN and concealed cycle length under P4 both before ($r=0.82$, $p<0.01$, $y=0.80x+104$) and after ($r=0.88$, $p<0.01$, $y=0.88x+102$) slow pathway ablation (not illustrated).

Comparison of Concealed vs. Conducted Beats Using Two Recovery Indexes

Recovery curves obtained with a conducted beat under P3 are compared to those obtained with concealed beats under P4 (Figure 7A). In that situation, atrial cycle length needs to be measured in a similar way whether the impulse is conducted or not. Therefore, the atrial cycle length associated with a concealed beat is measured as $A_1 \cdot A_0A_2$ while the cycle length associated with a conditioning conducted beat is measured as $A_1A_1 \cdot A_2$. Note that the recovery curve obtained with the longest cycle length (190-ms) closely matches the one obtained with the conditioning conducted impulse. In Figure 7B, the same conduction times are plotted against atrial cycle lengths measured as $A_1 \cdot A_2$ (P3) and A_0A_2 (P4). This excludes the conditioning and concealed cycles from the measurements. The recovery curves from the concealed beats became more tightly distributed near the control curve and slightly shifted leftward. The conditioning conducted beat still shifts the recovery curve to the right, but less than in Figure 7A.Therefore, the rightward shift of the recovery curve caused by concealed and conducted beats is highly dependent on the method used to assess atrial cycle length.

DISCUSSION

Our findings provide new insights into the determinants of the width of the concealment zone and of concealed conduction effects on slow and fast AV nodal pathway. First, our new approach with a conditioning cycle revealed a wide concealment zone in all preparations. Consequently, the effects of a broad range of concealed cycle lengths on nodal function could be explored. Secondly, we found that the pivotal effect of a concealed beat is to bodily shift the nodal recovery curve to the right proportionately to

concealed cycle length. ERPN and FRPN increased accordingly. Thirdly, we have established that, after slow pathway ablation, concealed conduction still causes a rightward shift of the fast pathway recovery curve, and increases ERPN and FRPN proportionately to concealed cycle length. In the aggregate, the effects of concealed conduction on AV nodal function are consistent with a resetting of the excitability cycle both in the slow and fast pathway.

Roles of Slow and Fast Pathway in AV Nodal Concealed Conduction

Does Partial Activation of Dual Pathways Account for Concealed Conduction?

The effects of concealed conduction on AV nodal function are commonly viewed as the result of a partial activation of AV node considered as a whole. Because the normal rabbit AV node contains both a slow and fast pathway,[18,19,23-25] the specific contribution of each pathway to concealed conduction needs to be assessed for a better understanding of the overall phenomenon. A central issue is whether the degree of partial activation and related block in slow and/or fast pathway are important determinants of concealed conduction effects on AV node. Our data on the effects of slow pathway ablation argue against that possibility. The fact that ablation did not prevent the rightward shift of the recovery curve indicates that partial activation of the slow pathway did not play a critical role in this phenomenon. In that situation, concealed cycles too short to be conducted through the fast pathway and obviously blocked in ablated slow pathway still produced significant rightward shift of the entire recovery curve (Figures 3 to 6 and Table 2). Moreover, concealed cycles tested before ablation were unavoidably shorter than ERPN of the slow pathway and yet caused a rightward shift of the entire recovery curve (slow + fast pathway) (Figures 3A and 4A). Thus, partial activation of the slow and/or fast pathway can unlikely account for concealed conduction effects. An alternate process needs to be invoked.

Dual Pathway Excitability Cycle and Concealed AV Nodal Conduction

Our search for an alternate explanation builds upon the well documented observation that the effects of concealed conduction depend on the timing of the concealed impulse within the concealment zone, a late pulse producing more effects than an early one.[2,4,6,13,28,29] Our findings extend that observation by more thoroughly characterizing the effects of concealed conduction on nodal recovery and refractory curves in the face of a wider concealment zone revealed by a conditioning cycle and/or slow pathway ablation. Increasing concealed cycle lengths led to major graded rightward shifts of the recovery curve. Despite these shifts, the curve shape was maintained and its asymptotic decay reached the same A_2H_2min. As far as the curve shape reflects recovery of nodal excitability,[30] concealed conduction reset but did not alter the excitability cycle. To account for concealed conduction effects, an excitability resetting would have to take place both proximally and distally to the site where the concealed beat is blocked, as suggested by others.[7,28,31,32] Transmembrane recordings clearly show that a concealed impulse initiates action potentials and thereby resets the excitability cycle in the proximal portion of the node.[2,33] The mechanism subtending excitability resetting in the portion of the node distal to the block is still not fully understood. Observations from a mathematical cable model of nodal myocytes predict that a concealed impulse may electrotonically trigger a partial activation of the transient calcium current ($I_{Ca.T}$)[7] thereby resetting the excitability cycle distally to the site of block. In agreement with that possibility, an electrotonic coupling exists between proximal and distal nodal cells[34,35] but its role in concealed conduction remains to be established. The fact that slow pathway ablation failed to alter concealed conduction effects suggests that the resetting takes place in the fast pathway.

Effects of a Concealed Beat on Slow Pathway Function

There is an apparent paradox between the failure of slow pathway ablation to modify the effects of concealed conduction on nodal curves and at the same time to

increase the width of the concealment zone. The window of cycle lengths belonging to slow pathway conduction before ablation is recruited to the concealment zone after ablation (Table 1). At identical concealed cycle lengths, the post ablation effects did not differ from the preablation ones. However, the possibility to test longer concealed cycle lengths after ablation led to greater concealed conduction effects. The integrity of slow pathway conduction was obviously not a determinant of these effects. Neither was the ablation essential to obtain major concealed conduction effects. In fact, the widest concealment zone and greatest concealed conduction effects were obtained with a conditioning cycle before ablation. This occurs without interfering with slow pathway conduction. The present findings show that, regardless of the width of the concealment zone, concealed conduction effects on nodal function primarily depend on concealed cycle lengths. Thus, the above paradox arises from the fact that ablation widens the concealment zone but does not directly increase concealed conduction effects.

Alternately, concealed conduction may interfere with slow pathway function. In humans, concealed impulses have been reported to mimic slow pathway ablation by reducing A_2H_2max.[16] This phenomenon was encountered in patients with and without typical broken recovery curves. Others have reported less consistent reductions of A_2H_2max.[15] In the present study, concealed conduction caused a slight decrease in mean A_2H_2max before ablation but statistical significance was not reached. Aside from species differences, other factors such as autonomic tone, stimulation protocols, and coupling interval resolution may contribute to this apparent discrepancy. Regardless of the effects of concealed conduction on A_2H_2max, our ablation data indicate that the slow pathway did not directly account for the effects of concealed conduction on nodal recovery curve. In fact, the primary effect of concealed conduction was to cause a rightward shift of the recovery curve irrespective of changes of A_2H_2max.

Assessment of Concealed Conduction Effects on Nodal Function: Analytical Biases

When assessing concealed conduction effects, the variables used to assess atrial cycle length and the selected reference baseline may have a major impact on conclusions reached. When the cycle length used to construct a nodal recovery curve is measured from an $A_1A_0A_2$ interval, A_1 marks the beginning of the nodal refractory cycle regardless of the presence of the concealed beat. This use of $A_1A_0A_2$ as a surrogate for A_1A_2 could be valid only if the concealed beat does not modify nodal recovery time. This is clearly incorrect for the nodal zone proximal to the block where the concealed impulse generates nodal action potentials and thereby resets the excitability cycle therein.[2,33] Consequently, recovery begins after A_0 rather than after A_1 in the portion of the node invaded by the concealed beat. If the nodal zone distal to the block is electrotonically reset by the concealed impulse, as discussed above, again A_0 rather than A_1 sets the beginning of recovery. When a conditioning cycle is included, $A_1A_0A_2$ becomes $A_1{\cdot}A_0A_2$ and the above reasoning still applies. As a consequence of using $A_1{\cdot}A_0A_2$ to assess nodal recovery time associated with a concealed beat, recovery curves are bodily shifted to the right together with ERPN. In contrast, the use of A_0A_2 to assess recovery time obliterates most of the effects displayed with $A_1{\cdot}A_0A_2$ (Figures 6D and 7B). Our comparison of $A_1{\cdot}A_0A_2$ and A_0A_2 clearly shows that the variable selected to measure atrial cycle length mitigates the impact of concealed conduction on the nodal recovery curve by changing its position on the x-axis (Figure 7). However, the shape of the nodal recovery curve is not modified by the selected variable, thereby reflecting the same recovery process.

The manner in which atrial cycle length is measured also had a major impact on ERPN. When measured from $A_1{\cdot}A_0A_2$, ERPN markedly increased with concealed cycle length ($A_1{\cdot}A_0$) (Figure 6A). We found that the inclusion of the concealed cycle length into ERPN measurements creates a bias largely accounting for the increase in ERPN (Figure 6C). The protocol-defined concealed cycle length then provides the x-axis value ($A_1{\cdot}A_0$) but, at the same time, equally contributes to y-axis value (ERPN) (Figure 6A).

Therefore, increases in A_1-A_0 will unavoidably augment ERPN (Figure 6C), irrespective of real changes in nodal refractoriness. Importantly, concealed beats only caused trivial changes in nodal refractoriness when assessed with A_0A_2 thereby excluding A_1-A_0 from measurements (Figure 6D).

The conditioning cycle alone (without concealed conduction) also had a clear impact on ERPN measurements. The augmented nodal conduction time of the conditioning beat itself caused a proportionate rightward shift of the refractory curve (Figures 5 and 6B). It is from this augmented ERPN that concealed conduction effects should be measured. The use of control ERPN as a reference to measure the effects of concealed conduction would neglect the fact that the conditioning cycle alone increases ERPN.

Implications

Our conditioning cycle approach may become a useful tool in the assessment of concealed conduction in humans. This particularly applies to patients who do not show a concealment zone under conventional protocols and may nonetheless display concealed conduction effects during tachyarrhythmias.[4,16] Our findings may also be relevant to the effects of slow pathway ablation/modification on ventricular response to atrial fibrillation in humans.[20-22] The fact that slow pathway ablation widens the concealment zone may explain the efficacy of this procedure to slow ventricular rate during atrial fibrillation. A widening of the concealment zone favors longer concealed cycle lengths and thereby greater concealed conduction effects. Because slow pathway ablation did not alter FRPN (Table 2), the minimum RR interval during atrial fibrillation should be maintained after ablation, as frequently observed. The unaltered FRPN may also explain the limited efficacy of slow pathway ablation to slow ventricular rate in the setting of rapid conducting atrial fibrillation.

Conclusions

Our new approach opens the way to thoroughly study the effects of concealed conduction on AV nodal function. The use of a conditioning cycle reveals a wide concealment zone consistently displayed in all preparations. The primary effect of concealed conduction is to cause a rightward shift of the entire nodal recovery curve, proportionate to concealed cycle length. ERPN and FRPN increase accordingly. Concealed beats may act as a resetting mechanism of slow and fast pathway excitability cycle similar to that expected from a conducted beat. Given that slow pathway ablation failed to prevent the effects of concealed conduction, the fast pathway is deemed to play a pivotal role in that process, presumably through electrotonic coupling. A resetting of excitability cycle rather than an impaired conduction or a prolonged refractoriness most likely accounts for AV nodal concealed conduction.

ACKNOWLEDGMENTS

The authors thank Lise Plamondon and Maurice Tremblay for their technical support, and Konstantinos Tzotzis for his comments on the manuscript.

REFERENCES

1. Langendorf R. Concealed A-V conduction: The effect of blocked impulses on the formation and conduction of subsequent impulses. Am Heart J 1948;35:542-552.
2. Moe G, Abildskov JA, Mendez C. An experimental study of concealed conduction. Am Heart J 1964;67:338-356.
3. Langendorf R, Pick A, Edelist A, Katz LN. Experimental demonstration of concealed AV conduction in the human heart. Circulation 1965;32:386-393.
4. Wu D, Denes P, Dhingra RC, Wyndham CR, Rosen KM. Quantification of human atrioventricular nodal concealed conduction utilizing S1S2S3 stimulation. Circ Res 1976;39:659-665.
5. Steinman RT, Lehmann MH. Beat-to-beat changes in atrioventricular nodal excitability and its modulation by concealed conduction during functional 2:1 block in man. Circulation 1987;76:759-767.
6. Chorro FJ, Sanchis J, Lopez-Merino V, Such L, Avellana JA, Valentin V. Effects of atrial impulse timing on AV concealed conduction in the rabbit heart. Pacing Clin Electrophysiol 1991;14:842-853.
7. Liu Y, Zeng W, Delmar M, Jalife J. Ionic mechanisms of electronic inhibition and concealed conduction in rabbit atrioventricular nodal myocytes. Circulation 1993;88:1634-1646.
8. Moe G, Abildskov JA. Observations on the ventricular dysrhythmia associated with atrial fibrillation in the dog heart. Circ Res 1964;14:447-460.
9. Langendorf R, Pick A, Katz LN. Ventricular response in atrial fibrillation. Role of concealed conduction in the A-V junction. Circulation 1965;32:69-75.
10. Moore EN. Observations on concealed conduction in atrial fibrillation. Circ Res 1967;21:201-208.

11. Cohen SI, Lau SH, Berkowitz WD, Damato AN. Concealed conduction during atrial fibrillation. Am J Cardiol 1970;25:416-419.
12. Toivonen L, Kadish A, Kou W, Morady F. Determinants of the ventricular rate during atrial fibrillation. J Am Coll Cardiol 1990;16:1194-1200.
13. Fujiki A, Tani M, Mizumaki K, Yoshida S, Sasayama S. Quantification of human concealed atrioventricular nodal conduction: relation to ventricular response during atrial fibrillation. Am Heart J 1990;120:598-603.
14. Brugada P, Roy D, Weiss J, Dassen WR, Wellens HJ. Dual atrio-ventricular nodal pathways and atrial fibrillation. Pacing Clin Electrophysiol 1984;7:240-247.
15. Lee PC, Wu JM, Wolff GS, Young ML. Effects of a blocked atrial beat on the atrioventricular nodal recovery property in patients with dual nodal pathways. Pacing Clin Electrophysiol 2003;26:2091-2095.
16. Liu S, Olsson SB, Yang Y, Hertervig E, Kongstad O, Yuan S. Concealed conduction and dual pathway physiology of the atrioventricular node. J Cardiovasc Electrophysiol 2004;15:144-149.
17. Billette J. Anatomy and physiology of concealment in dual atrioventricular nodal pathways. J Cardiovasc Electrophysiol 2004;15:150-152.
18. Zhang Y, Bharati S, Mowrey KA, Mazgalev TN. His electrogram alternans reveal dual atrioventricular nodal pathway conduction during atrial fibrillation: the role of slow-pathway modification. Circulation 2003;107:1059-1065.
19. Zhang Y, Bharati S, Sulayman R, Mowrey KA, Tchou PJ, Mazgalev TN. Atrioventricular nodal fast pathway modification: mechanism for lack of ventricular rate slowing in atrial fibrillation. Cardiovasc Res 2004;61:45-55.
20. Feld GK, Fleck RP, Fujimura O, Prothro DL, Bahnson TD, Ibarra M. Control of rapid ventricular response by radiofrequency catheter modification of the atrioventricular node in patients with medically refractory atrial fibrillation. Circulation 1994;90:2299-2307.

21. Williamson BD, Man KC, Daoud E, Niebauer M, Strickberger SA, Morady F. Radiofrequency catheter modification of atrioventricular conduction to control the ventricular rate during atrial fibrillation. N Engl J Med 1994;331:910-917.
22. Morady F, Hasse C, Strickberger SA, Man KC, Daoud E, Bogun F, Goyal R, Harvey M, Knight BP, Weiss R, Bahu M. Long-term follow-up after radiofrequency modification of the atrioventricular node in patients with atrial fibrillation. J Am Coll Cardiol 1997;29:113-121.
23. Medkour D, Becker AE, Khalife K, Billette J. Anatomic and functional characteristics of a slow posterior AV nodal pathway: role in dual-pathway physiology and reentry. Circulation 1998;98:164-174.
24. Khalife K, Billette J, Medkour D, Martel K, Tremblay M, Wang J, Lin LJ. Role of the compact node and its posterior extension in normal atrioventricular nodal conduction, refractory, and dual pathway properties. J Cardiovasc Electrophysiol 1999;10:1439-1451.
25. Reid MC, Billette J, Khalife K, Tadros R. Role of compact node and posterior extension in direction-dependent changes in atrioventricular nodal function in rabbit. J Cardiovasc Electrophysiol 2003;14:1342-1350.
26. Billette J. What is the atrioventricular node? Some clues in sorting out its structure-function relationship. J Cardiovasc Electrophysiol 2002;13:515-518.
27. Efimov IR, Nikolski VP: Mechanisms of AV nodal excitability and propagation. In: Zipes DP, Jalife J, editors. *Cardiac Electrophysiology From Cell to Bedside*. Philadelphia: Saunders, 2004: 203-212.
28. McKinnie J, Avitall B, Caceres J, Jazayeri M, Tchou P, Akhtar M. Electrophysiologic spectrum of concealed intranodal conduction during atrial rate acceleration in a model of 2:1 atrioventricular block. Circulation 1989;80:43-50.
29. van Capelle FJL, Du Perron J, Durrer D. Atrioventricular conduction in isolated rat heart. Am J Physiology 1971;221:284-290.

30. Merideth J, Mendez C, Mueller WJ, Moe GK. Electrical excitability of atrioventricular nodal cells. Circ Res 1968;23:69-85.
31. Antzelevitch C, Moe GK. Electrotonic inhibition and summation of impulse conduction in mammalian Purkinje fibers. Am J Physiol 1983;245:H42-H53.
32. Meijler FL, Jalife J, Beaumont J, Vaidya D. AV nodal function during atrial fibrillation: the role of electrotonic modulation of propagation. J Cardiovasc Electrophysiol 1996;7:843-861.
33. Mendez C, Moe GK. Some characteristics of transmembrane potentials of AV nodal cells during propagation of premature beats. Circ Res 1966;19:933-1010.
34. Billette J, Janse MJ, van Capelle FJ, Anderson RH, Touboul P, Durrer D. Cycle-length-dependent properties of AV nodal activation in rabbit hearts. Am J Physiol 1976;231:1129-1139.
35. Billette J. Atrioventricular nodal activation during periodic premature stimulation of the atrium. Am J Physiol 1987;252:H163-H177.

LEGENDS

Figure II-1

A, preparation with landmarks, pacing site (square wave), recording sites (small circles), and slow pathway ablation site (large circles). B, protocols as ladder diagrams of atrial and His bundle activation times. P1, control protocol. P2, concealed conduction protocol in which the concealed A_1A_0 cycle results in a blocked A_0 beat. P3, conditioning cycle protocol in which a conditioning $A_1A_{1'}$ cycle 10-ms longer than control ERPN results in a conducted $A_{1'}$ beat. P4, combined effects of a conditioning and concealed cycle protocol. The subscripts mark beats as defined in the insert box. CFB = central fibrous body; CN = compact node; CS = coronary sinus; CT = crista terminalis; IAS = interatrial septum; PNE = posterior nodal extension; TT = tendon of Todaro; TV = tricuspid valve; UA = upper atrium.

Figure II-2

Concealment zone with and without a conditioning cycle before and after slow pathway ablation. Data are reported as mean±SD for P1 (closed circles) and P3 (open circles). SD = standard deviation; NS = not statistically significant.

Figure II-3

A, recovery curves obtained at control (P1) and with a concealed cycle (P2) before ablation in one preparation. Concealed conduction causes a rightward shift of the entire curve with trivial effects on A_2H_2max. B, curves obtained with P1 and P2 after ablation. Ablation reduces A_2H_2max and slightly increases the rightward shift of the curves caused by the concealed beats.

Figure II-4

A, effects of a conditioning cycle on nodal recovery curves obtained at control (P1) and at different concealed cycle lengths (P4) before slow pathway ablation in same preparation as in Figure 3. Increasing concealed cycle length caused graded rightward shifts of the nodal recovery curve. B, nodal curves obtained with P1 and P4 after ablation.

Ablation reduces A_2H_2max in all curves. The shortened concealed cycle range results in reduced but still definite rightward shift of nodal recovery curves.

Figure II-5

Effects of concealed cycle lengths (A_1A_0 or $A_1{\cdot}A_0$) with and without a conditioning cycle ($A_1A_1{\cdot}$), before (A) and after (B) slow pathway ablation on refractory curves in same preparation as in Figures 3 and 4 (symbols correspond). Only concealed conduction curves corresponding to minimum and maximum concealed cycle length are shown. In upper panel, the conditioning cycle alone bodily shifts the curves to the right and thereby alters the baseline from which the effects of concealed conduction are referenced. In lower panel, concealed conduction still shifted the curves rightward but less than in A because of a longer conditioning cycle after ablation. AA corresponds to A_1A_2 (P1), $A_1A_0A_2$ (P2), $A_1A_1{\cdot}A_2$ (P3) or $A_1{\cdot}A_0A_2$ (P4), as defined in Figure 1B. HH corresponds to H_1H_2 (P1 and P2) or $H_1{\cdot}H_2$ (P3 and P4).

Figure II-6

Factors contributing to concealed conduction effects on ERPN values obtained under P4. A, linear relations between the concealed cycle length ($A_1{\cdot}A_0$) and ERPN before (closed circles, $r=0.97$, $p<0.01$, $y=1.2x+67$) and after (open circles, $r=0.91$, $p<0.01$, $y=1.1x+72$) ablation. B, linear relation between the increase in conduction time of the conditioning beat ($\Delta A_1{\cdot}H_1{\cdot}$) over that of the control beat and rightward shift of refractory curves (before $r=0.99$, $p<0.01$, $y=x+1$ and after ablation $r=0.99$, $p<0.01$, $y=x$). C, linear relation between $A_1{\cdot}A_0$ at ERPN and protocol-imposed $A_1{\cdot}A_0$. Note that imposed concealed cycle length equally contributes to both axes of the graph. D, weak relation between A_0A_2 at ERPN and concealed cycle length before ($r=0.51$, $p<0.02$, $y=0.2x+68$) and after ablation ($r=0.27$, NS, $y=0.15x+72$). In all panels, data points obtained before and after slow pathway ablation overlap and share a similar slope.

Figure II-7

Comparison of effects of concealed and conducted beats on nodal recovery curves using two recovery indexes. A, comparison of recovery curves from different concealed cycle lengths (P4, same as in Figure 4A) to that from a conducted conditioning cycle (P3). A similar approach is used to measure atrial cycle length in concealed (A_1'A_0A_2) and conducted (A_1A_1'A_2) beats. Note that the curve obtained for the 190-ms concealed cycle length (close downward arrowheads) closely parallels that of the conducted conditioning cycle (open downward arrowheads). B, same A_2H_2 data plotted against atrial cycle lengths measured as A_1A_2 at control, A_0A_2 after a concealed cycle or A_1'A_2 after a conditioning cycle.[4-6,15] Note that the recovery curves from concealed beats were no longer shifted to the right of control. However, the curve from the conditioning cycle remains partially shifted to the right.

Table 1 Effects of a conditioning cycle and/or slow pathway ablation on lower and upper limit of AV nodal concealment zone.

	Before Ablation		After Ablation	
Conditioning Cycle	−	+	−	+
Lower Limit	81±5	86±11	86±7	81±7
Upper Limit	103±9	163±44†	131±16‡	148±11*§‖

Values are mean±SD in ms, n=6 except for 1st column of data where n=3. Upper vs. lower limit values differ systematically ($p \leq 0.01$). Lower limit values do not differ significantly between each others. * $p \leq 0.01$, † $p \leq 0.02$, ‡ $p \leq 0.03$ compared to value obtained before ablation without a conditioning cycle; § $p \leq 0.02$ compared to value obtained without a conditioning cycle after ablation. ‖ NS compared to value obtained with a conditioning cycle before ablation.

Table 2 Effects of concealed conduction on ERPN and FRPN before and after ablation in data obtained with a conditioning cycle.

	Before Ablation				After Ablation			
	P1	**P3**	**P4min**	**P4max**	**P1**	**P3**	**P4min**	**P4max**
ERPN	100±8	163±44	175±29	263±34	131±16*	148±11†	175±23†	233±17†
FRPN	175±15	160±21	173±19	239±25	175±14†	162±16†	186±21†	246±10†

	P values of statistical comparisons					
	P3 vs. P1	**P4min vs. P1**	**P4max vs. P1**	**P4min vs. P3**	**P4max vs. P3**	**P4max vs. P4min**
ERPN						
Before Ablation	0.01	0.01	0.01	NS	0.01	0.01
After Ablation	NS	0.01	0.01	0.02	0.01	0.01
FRPN						
Before Ablation	0.01	NS	0.01	NS	0.01	0.01
After Ablation	0.01	0.03	0.01	0.01	0.01	0.01

Top 2 row values are mean±SD in ms, n=6. P1, P3 and P4 correspond to protocols. P4min and P4max correspond to values obtained at minimum and maximum concealed cycle length, respectively. * $p<0.01$, † not statistically significant comparing values after vs. before ablation.

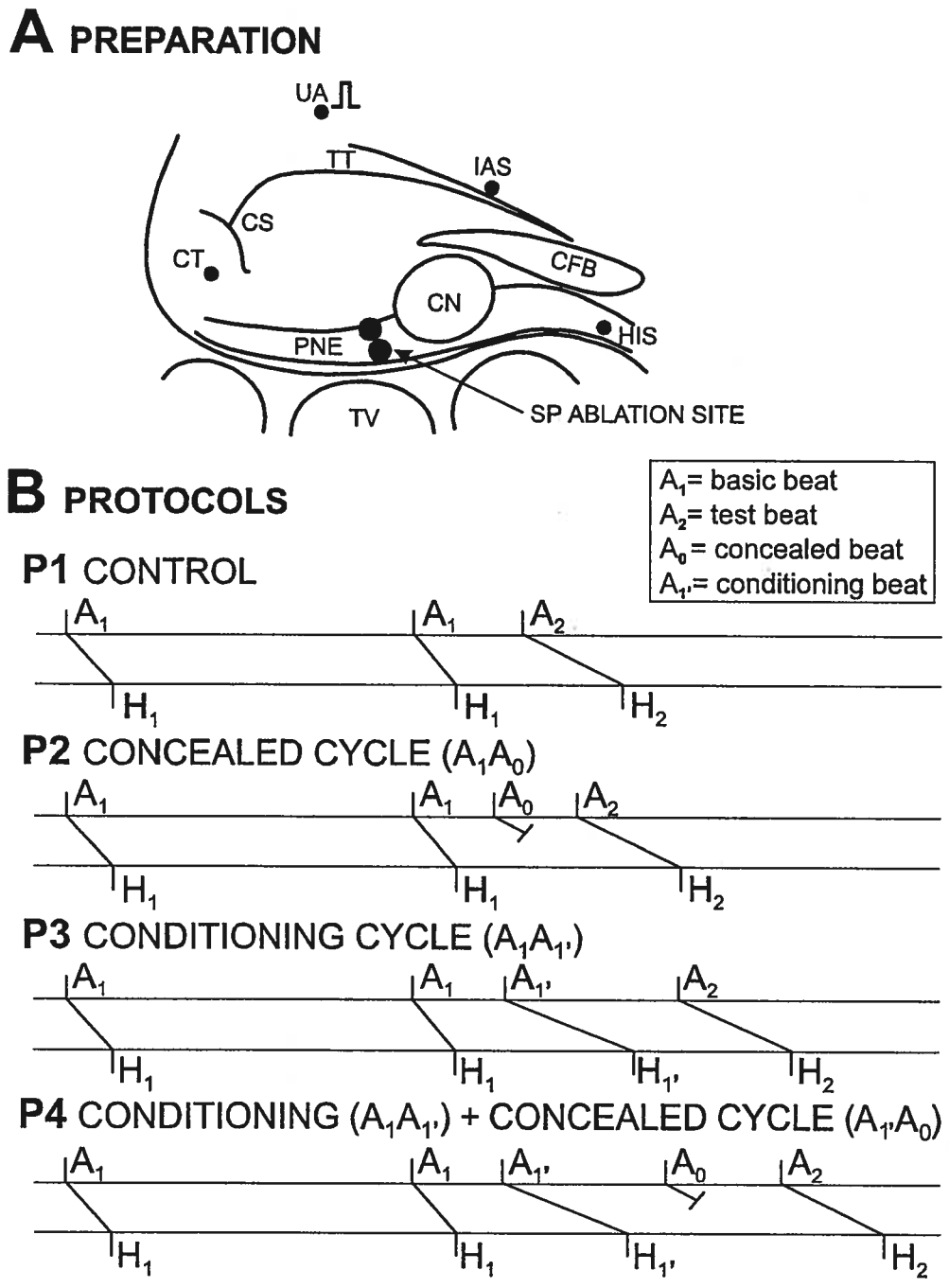
A PREPARATION
UA
TT
IAS
CS
CT
CFB
CN
HIS
PNE
TV
SP ABLATION SITE
B PROTOCOLS
A1= basic beat
A2= test beat
A0= concealed beat
A1'= conditioning beat
P1 CONTROL
P2 CONCEALED CYCLE (A1A0)
P3 CONDITIONING CYCLE (A1A1')
P4 CONDITIONING (A1A1') + CONCEALED CYCLE (A1'A0)

Figure II-1

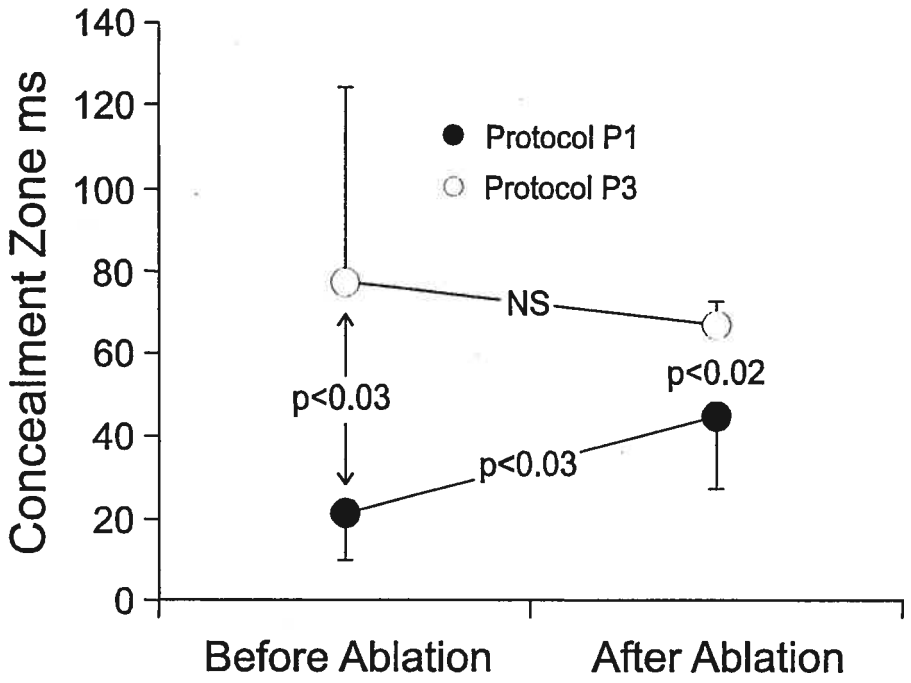
140
120
100
80
60
40
20
0
Concealment Zone ms
Protocol P1
Protocol P3
NS
p<0.03
p<0.02
p<0.03
Before Ablation
After Ablation

Figure II-2

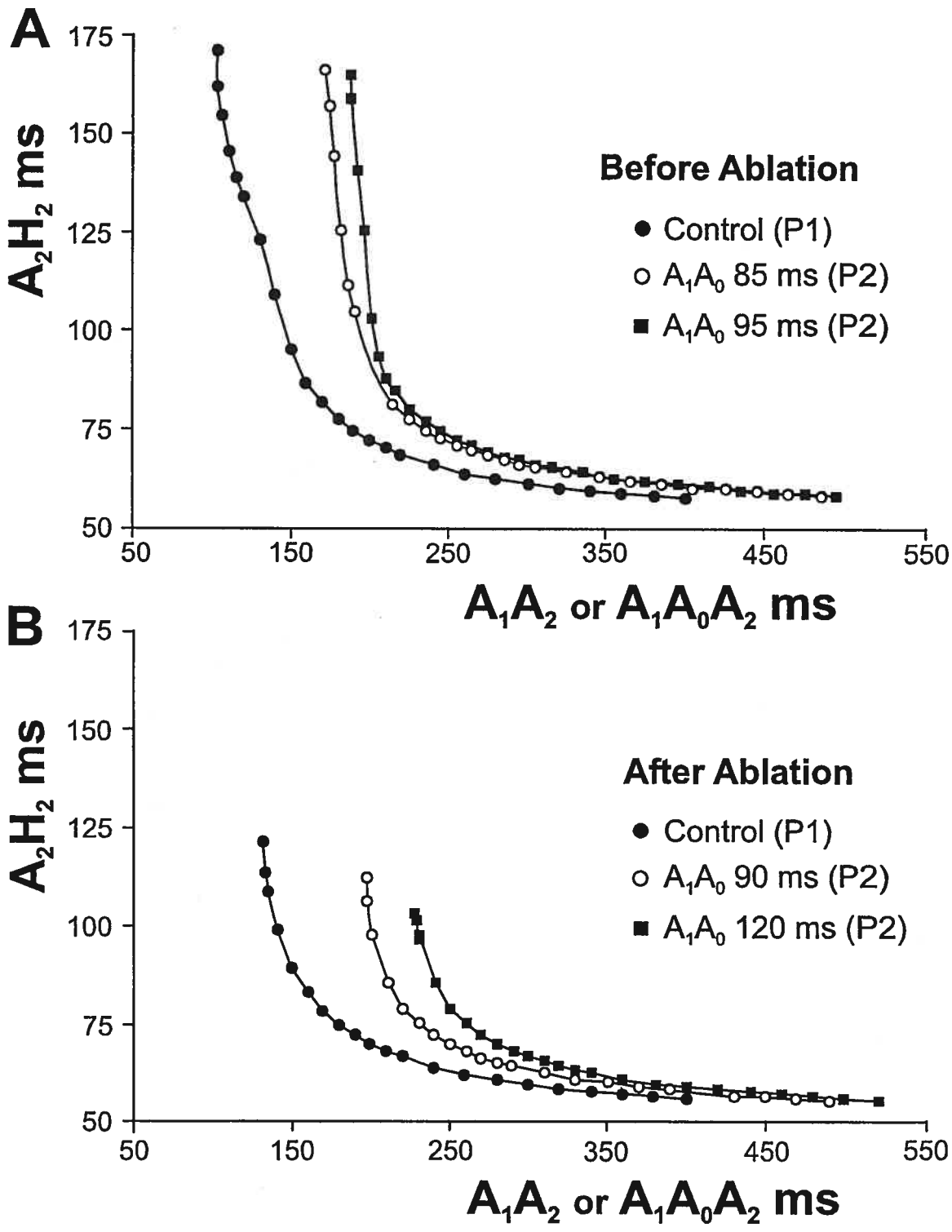
A
A_2H_2 ms
175
150
125
100
75
50
50
150
250
350
450
550
A_1A_2 or $A_1A_0A_2$ ms
Before Ablation
Control (P1)
A_1A_0 85 ms (P2)
A_1A_0 95 ms (P2)
B
A_2H_2 ms
175
150
125
100
75
50
50
150
250
350
450
550
A_1A_2 or $A_1A_0A_2$ ms
After Ablation
Control (P1)
A_1A_0 90 ms (P2)
A_1A_0 120 ms (P2)

Figure II-3

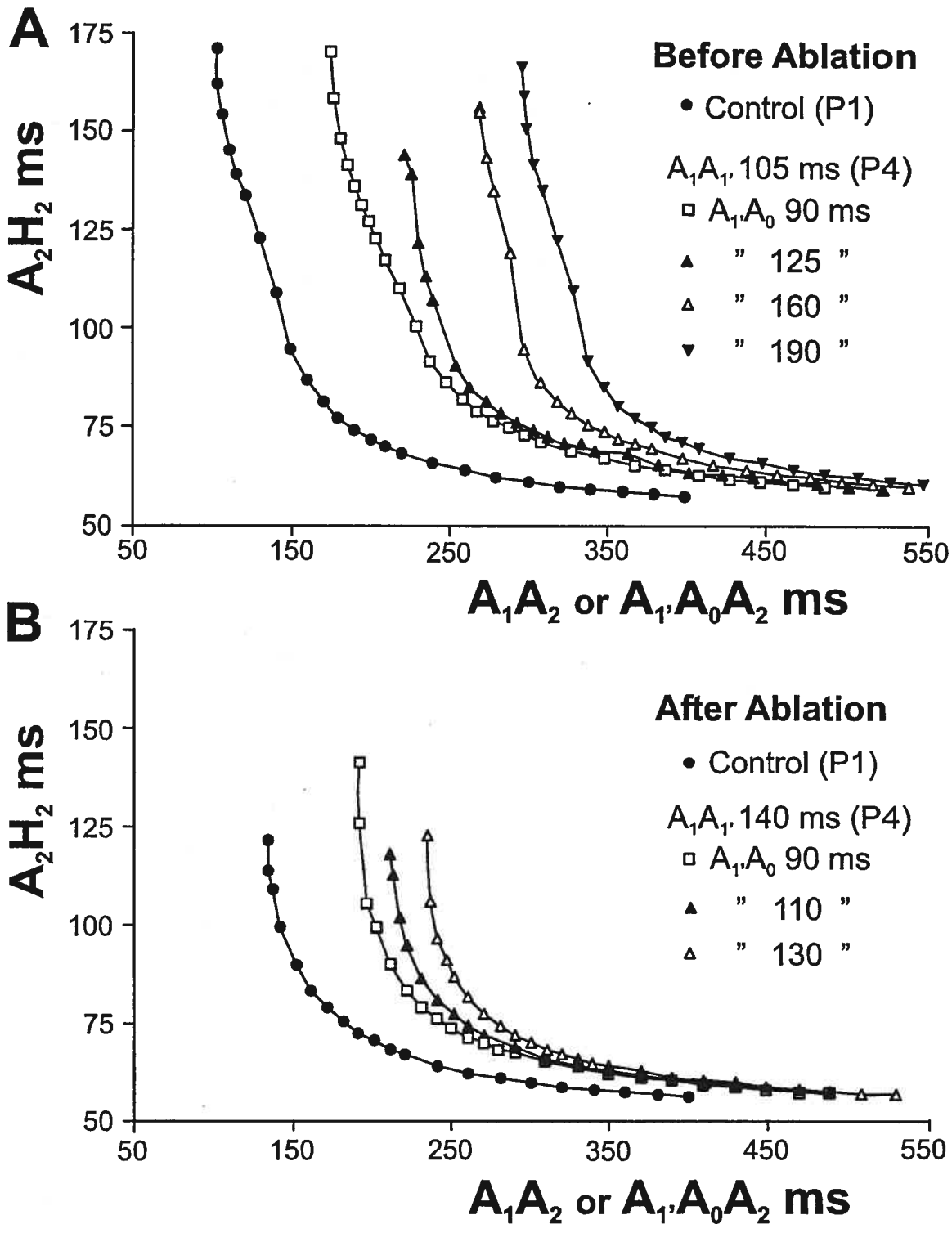
A
Before Ablation
• Control (P1)
A1A1, 105 ms (P4)
□ A1,A0 90 ms
▲ " 125 "
△ " 160 "
▼ " 190 "
A2H2 ms
175
150
125
100
75
50
50
150
250
350
450
550
A1A2 or A1,A0A2 ms
B
After Ablation
• Control (P1)
A1A1, 140 ms (P4)
□ A1,A0 90 ms
▲ " 110 "
△ " 130 "
A2H2 ms
175
150
125
100
75
50
50
150
250
350
450
550
A1A2 or A1,A0A2 ms

Figure II-4

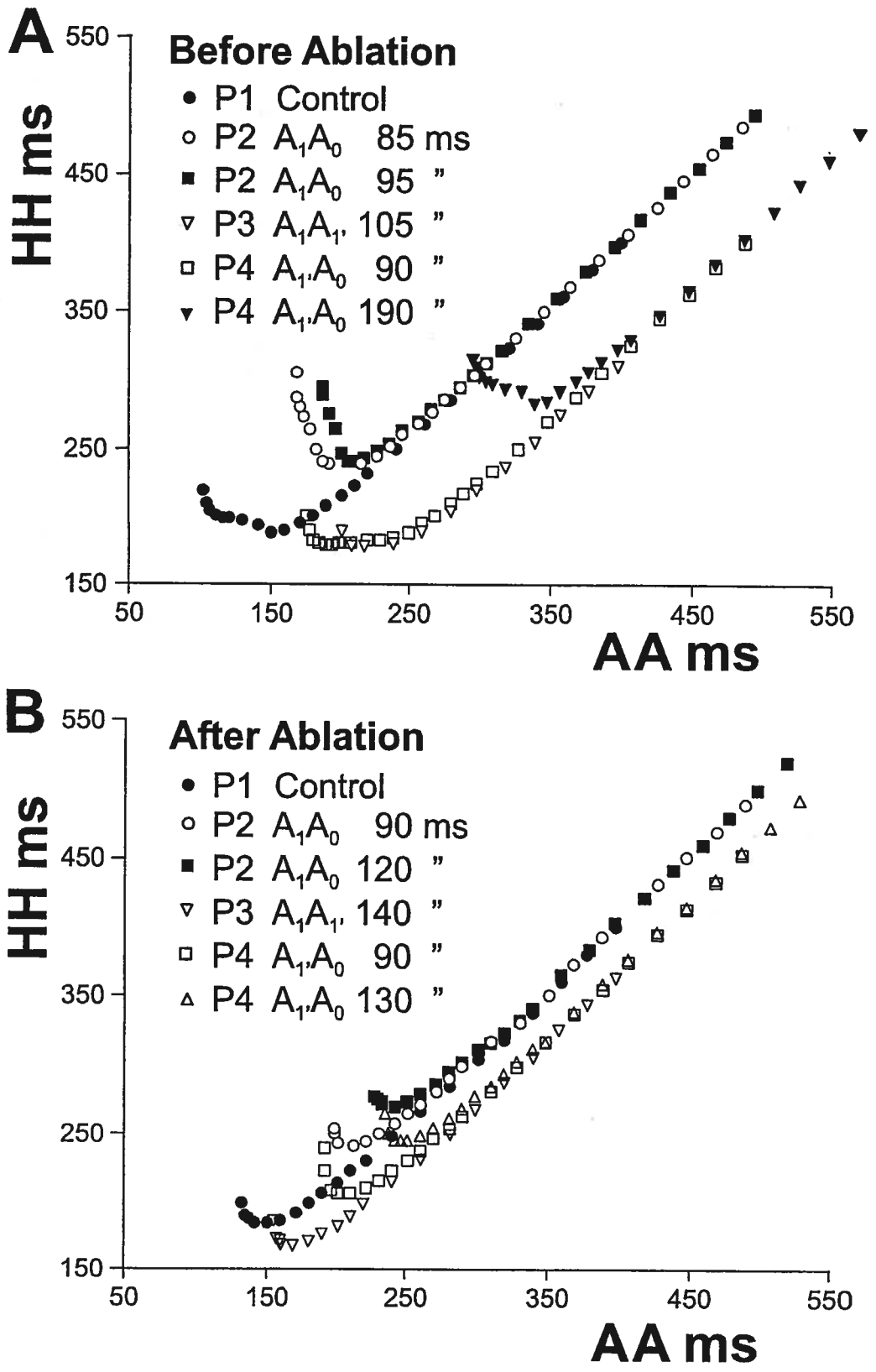
A
Before Ablation
P1 Control
P2 A1A0 85 ms
P2 A1A0 95 "
P3 A1A1 105 "
P4 A1A0 90 "
P4 A1A0 190 "
HH ms
AA ms
550
450
350
250
150
50
150
250
350
450
550
B
After Ablation
P1 Control
P2 A1A0 90 ms
P2 A1A0 120 "
P3 A1A1 140 "
P4 A1A0 90 "
P4 A1A0 130 "
HH ms
AA ms

Figure II- 5

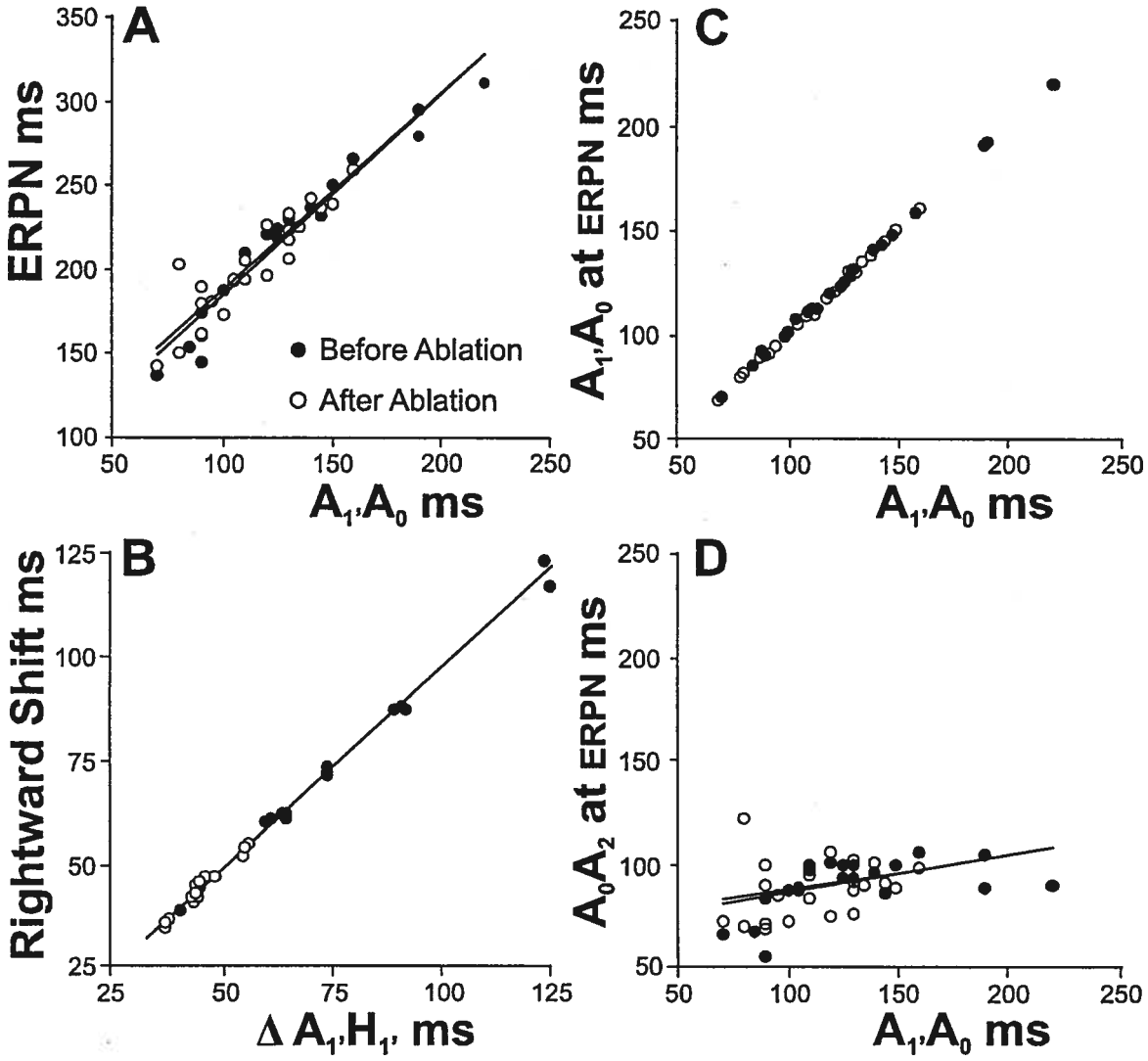
A
ERPN ms
A_1,A_0 ms
Before Ablation
After Ablation
B
Rightward Shift ms
$\Delta A_1,H_1$, ms
C
A_1,A_0 at ERPN ms
A_1,A_0 ms
D
A_0A_2 at ERPN ms
A_1,A_0 ms

Figure II-6

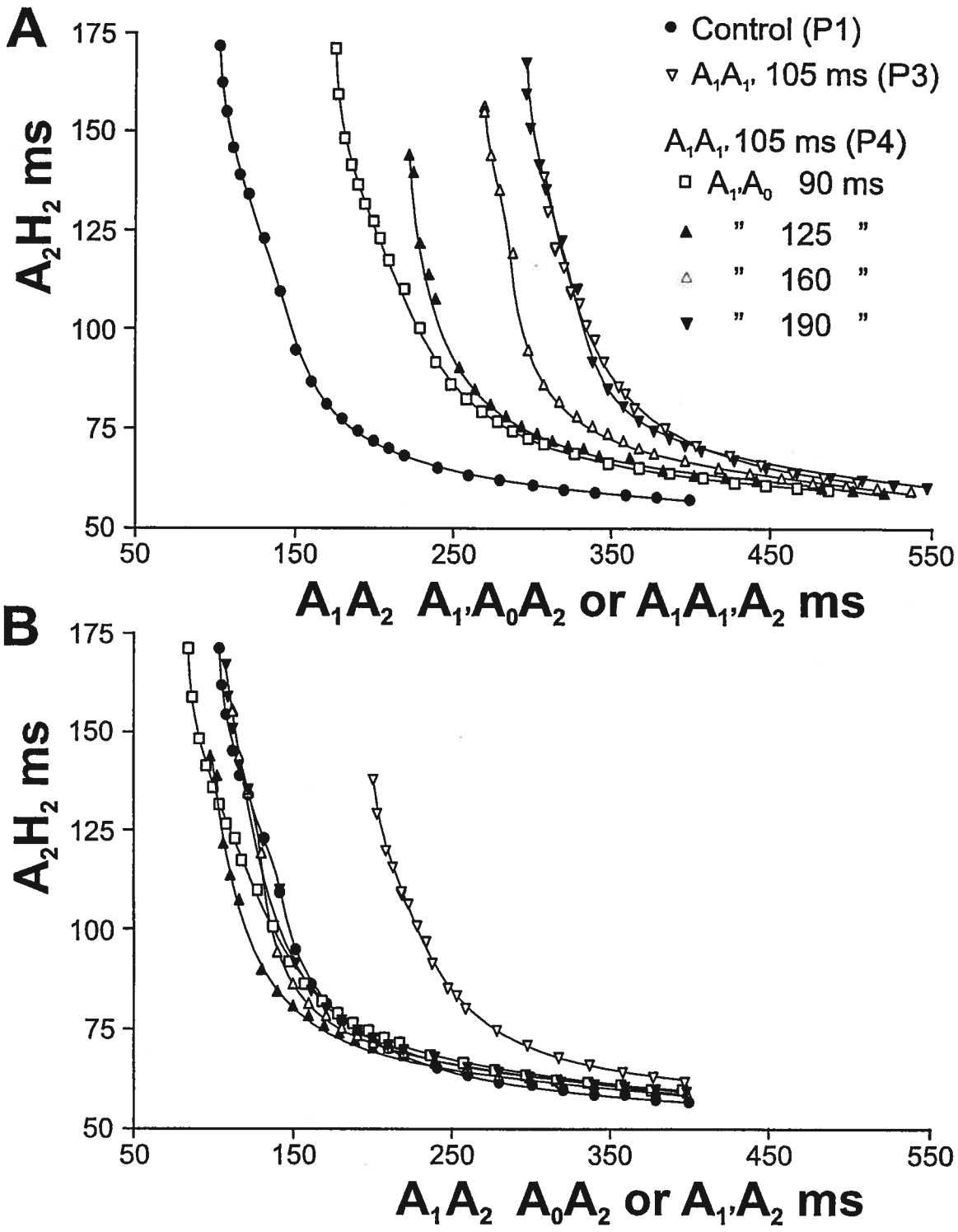
A
B
Control (P1)
A1A1, 105 ms (P3)
A1A1, 105 ms (P4)
A1,A0 90 ms
" 125 "
" 160 "
" 190 "
A2H2 ms
A1A2 A1,A0A2 or A1A1,A2 ms
A1A2 A0A2 or A1,A2 ms
175
150
125
100
75
50
50
150
250
350
450
550

Figure II-7

CHAPTER III: GENERAL DISCUSSION

Main new findings

The present findings provide new insight into the understanding of concealed conduction in normal dual pathway rabbit AV node. The protocols allowed for the determination of the concealment zone and of the effects of different concealed cycles chosen within the concealment zone. When this was done with the standard protocol, i.e., a concealed A_0 beat introduced between the last basic A_1 beat and test A_2 beat, the concealment zone was narrow and inconsistent so that concealed cycle lengths could be inconsistently tested only over a narrow range. Increasing the concealed cycle length within this narrow range resulted in proportional rightward shift of the nodal recovery curve and increase both ERPN and FRPN. This occurred without affecting the shape of the curve. To overcome the difficulties associated to a narrow and inconsistent zone of concealment, we developed a protocol in which a conditioning A_1' beat is introduced before each concealed A_0 beat (Figure II-1B). This new approach resulted in a markedly broaden and consistent concealment zone and accordingly increased the range of concealed cycle lengths that could be tested. The A_1' beat increased only the upper limit of the concealment zone, the lower limit remaining virtually unchanged. In these conditions, the rightward shift of the nodal recovery curve, ERPN and FRPN increased further with the concealed cycle length. However, these greater effects occurred over the same linear relationship than observed with narrower ranges of concealed cycle lengths. In other words, the effects were greater but their dependence on concealed cycle length remained unchanged. The slow pathway ablation also broadened and made the concealment zone consistent but did not alter the relationship to concealed cycle length.

The effects of A_1' beat and ablation were independent and non-additive. Regardless of prevailing pathway and/or the presence or not of A_1' beat, ERPN increased linearly with concealed cycle length along the same relationship (Figure II-6). However, we found that the ERPN increase was closely tied to the prolongation of A_1'H_1' and of imposed A_1'A_0 and thus reflected more measurement artefacts than real changes in nodal refractoriness. In fact, A_1'A_0 is the imposed concealed cycle length and thus cannot be an index of nodal refractoriness. Its inclusion in ERPN measurements biases ERPN measurements and thereby the apparent effects of concealed conduction on ERPN. When this bias is eliminated by measuring ERPN with A_0A_2, we found that ERPN increases very slightly with concealed cycle length. The ablation increased ERPN measured in either manner but did not alter its linear relationship to concealed cycle length.

The findings also show that the baseline of the refractory curve is bodily shifted to a longer cycle length range by a conditioning cycle in proportion to A_1'H_1' prolongation (Figure II-5B). In data obtained without a conditioning cycle, this baseline corresponded to the identity line where H_1'H_2 and A_1'A_2 are equal. Due to the increase in A_1'H_1', any given H_1'H_2 occurs necessarily at a longer A_1'A_0 A_2 that accordingly shifts the baseline to the right. This prolongs ERPN causing A_1'A_0 effects on ERPN to occur from a prolonged value. Another important observation was that concealed conduction does not consistently prevent slow pathway conduction; concealed cycle length did not significantly affect A_2H_2max before ablation and tended to increase it after ablation. All above findings are compatible with an excitability resetting arising from an electronic interaction between the zone proximal and distal to the concealed block site. This explanation is more thoroughly given in the manuscript and thus will not be repeated.

Because the concealed beat resets the excitability cycle by a direct activation in the zone proximal to the block and may do so electrotonically in distal portion, the question arises of whether the recovery cycle preceding the test beat after a concealed beat should be measured by the longest non conducted $A_1A_0A_2$ as done in present and many other studies or by A_0A_2.[97,131,152-154] This also applies to ERPN. In trying to make sense out of ERPN changes without $A_1{\cdot}A_0$ and $A_1{\cdot}H_1{\cdot}$ biases, we discuss further below the effects of concealed conduction on ERPN as assessed from A_0A_2.

Meaning of concealed-conduction-induced changes in nodal recovery and refractory curves

The different and even opposite results of concealed conduction on the nodal recovery curves constructed as A_2H_2 vs. A_0A_2 and A_2H_2 vs. $A_1{\cdot}A_0A_2$ are puzzling (Figure II-7). In the A_2H_2 vs. A_0A_2 curves of Figure II-7B, there is no rightward shift to be seen, as was the case with $A_1{\cdot}A_0A_2$ curves (Figure II-7A). Curves even appear to be slightly shifted to the left of the control curve in the short coupling interval range, an apparent facilitatory effect. The shift associated to the conditioning cycle alone remains rightward but is reduced. The disappearance of rightward shift in Figure II-7B is clearly associated to the removal of $A_1{\cdot}A_0$ from the atrial cycle length. The persistence of some rightward shift in the curve associated to the conditioning cycle may be attributed to the long $A_1{\cdot}H_1{\cdot}$ that, as for the refractory curve, shifted the recovery curve to a longer $A_1{\cdot}A_0A_2$ range than the control A_1A_2 one. Notably, when ERPN is measured from longest non conducted A_0A_2, it increases only slightly with increasing cycle length but does so from an initially shortened value as compared to control (Figure II-7D). This result suggests that ERPN is less and less shortened by the concealed beat as concealed cycle length increases. As shown in Figure III-1, the progressive increase in leftward shift of the recovery curve

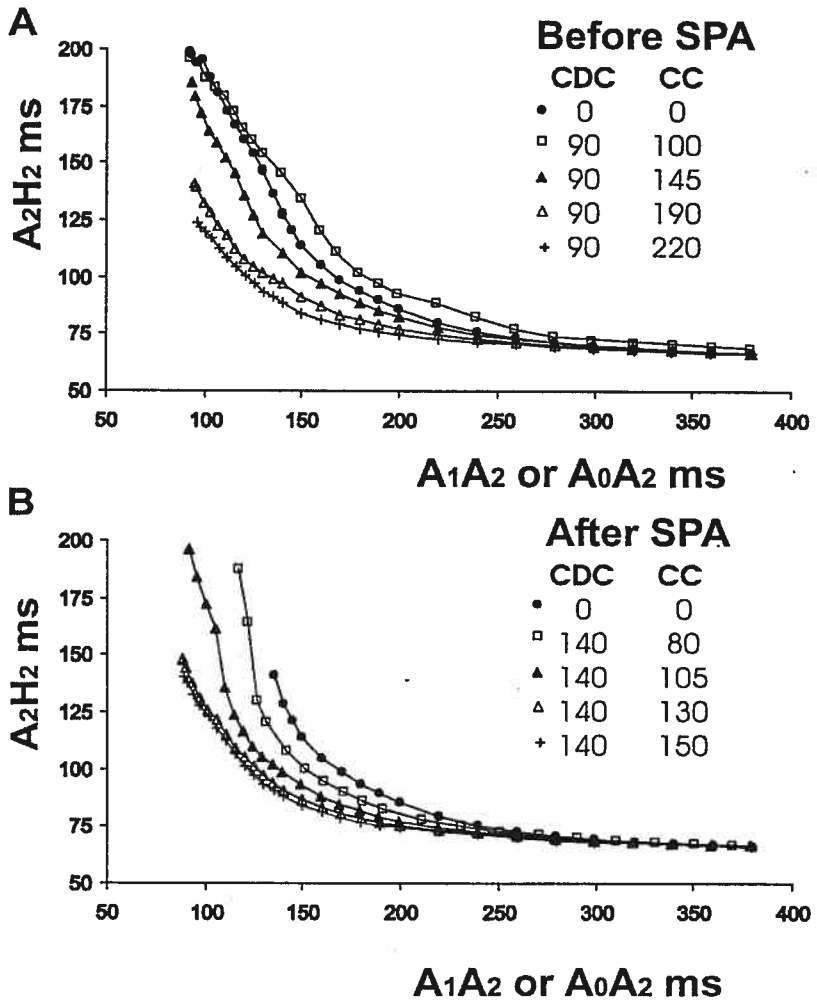

Figure III-1 Leftward shift, in reference to control, of A_2H_2 vs. A_0A_2 AV nodal recovery curve induced by concealed cycles tested with a conditioning cycle before (A) and after (B) slow pathway ablation in one preparation. The shift increases with concealed cycle length both before and after slow pathway ablation.

observed before ablation (panel A) persists after ablation (panel B). This result indicates that these leftward shifts are independent of the integrity of the slow pathway. Further studies will be necessary to sort out the precise significance of these findings.

The electrotonic effects of the concealed beat upon the zone distal to the block are postulated by several studies.[140,151,155,156] However, the exact nature of the electrotonic

events that took place in the present study are not known. As far as could be appreciated by the effects of all concealed beats studied that shifted the entire curve to the right without altering its shape, it is clear that the distal node ought to be involved. The absence of electrotonic effects would have resulted in no effects on the curve in long A_1'A_0A_2 range; in both the control and concealed conduction curve, the node would be recovering in the same manner in distal node from A_1' activation, events that should be reflected by overlapping curves. This was not the case.

Another observation not included in the manuscript concerns mean changes in ERPN measured from A_0A_2. Before slow pathway ablation, this ERPN remained relatively constant whether a conditioning cycle was present or not (91±12 ms at control, 86±13 ms under maximum concealed conduction effects, and 93±9 ms with conditioning cycle plus concealed conduction). After slow pathway ablation, concealed conduction increased ERPN to 105±1 ms but not when tested in association with a conditioning cycle (90±2 ms). Moreover, the effects of increasing concealed cycle length on this ERPN measurement were minimal and at the limit of significance. These results contrast with those obtained when ERPN measurement include A_1'A_0 and suggest that concealed conduction would in fact have very little real effects on nodal refractoriness.

The postulated electrotonic effect is unlikely to be an all or none one. When an impulse penetrates the node but fails to traverse it completely, at one point it becomes subthreshold for cells located distal to the block site. This subthreshold event does not vanish abruptly but likely results in a decreasing electrotonic depolarization that depends on distance, membrane resistance, and degree of electrical coupling among cells. These graded decreasing subthreshold electrotonic potentials are likely to have different effects

along their non conducting path. A possibility would be a corresponding decrement in the transient calcium current ($I_{Ca.T}$) in nodal cells increasingly more distal to the block.[151] Another could be an easier depolarization by the test beat when the concealed beat partially depolarizes the cell without making it refractory. Obviously, our results do not allow us to assess these possibilities and their eventual involvement in facilitatory effects of a concealed beat upon conduction and ERPN.

Several studies have interpreted as impairing effects of concealed conduction on nodal function the differences in A_2H_2 observed at comparable cycle lengths. The superimposition of A_2H_2 vs. $A_1A_0A_2$ and A_2H_2 vs. A_1A_2 curve indeed shows that, at any corresponding $A_1A_0A_2$ and A_1A_2, A_2H_2 is longer in the presence of the concealed beat. This apparent effect increases with concealed cycle length. As this effect may be equivalent to that of a barely conducted beat (Figure II-7A) and vanishes when A_1A_0 is taken out from atrial cycle length, it is likely that this effect is largely a measurement bias associated to the use of $A_1A_0A_2$ as index of atrial cycle length.

Interestingly, both formats result in identical curve shape i.e., similarly reflect the recovery from nodal activation. This similarity indicates that they cannot be attributed to a difference in nodal functional state. This observation also suggests that the two formats reflect in the same manner the concealed-conduction-induced resetting of excitability.

Site of nodal delay and action potential characteristics

In addition to facilitatory effects in short coupling interval range, the A_2H_2 vs. A_0A_2 curve shows another interesting phenomenon. The extent of this leftward shift and/or tilt with respect to the control curve does not always increase with concealed cycle length (Figure III-2). Usually, with the increase of concealed cycle length, the curves affected by concealed conduction is shifted to the left of the control one. However, the curve

obtained at maximum concealed cycle length was sometimes located at intermediate degrees of shifts. This was observed both before and after slow pathway ablation with or

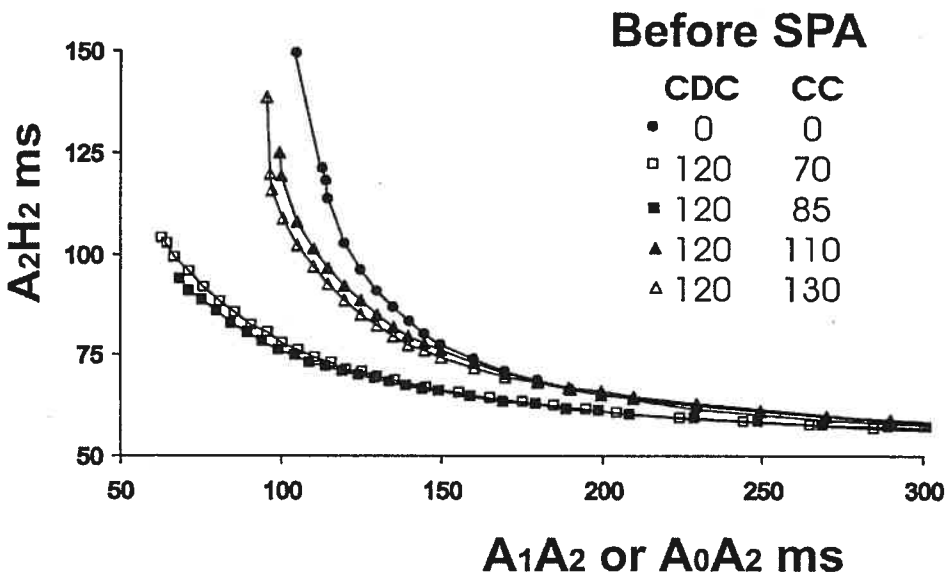

Figure III-2. Effects of a conditioning and concealed cycle on AV nodal recovery curves obtained before slow pathway ablation in one preparation. Superimposed curves show that increasing concealed cycle length induces a biphasic leftward tilt/shift of curve. As concealed cycle length increased, the tilt/shift first increased and then decreased with respect to the control curve.

without conditioning cycle. We suggest that this variation may arise from the fact that the recovery curve has a complex origin in the node.

The recovery-dependent increase in conduction delay represented by the recovery curve is indeed a complex phenomenon (Figure III-3).[38] The proximal nodal cells, including the N cells, account for 21% of the mean nodal delay at longest cycle length. This contribution remains unchanged over a wide range of decreasing coupling intervals to increase only slightly in very short ones. On this basis, one may speculate that, during the broad concealment zone obtained with a conditioning cycle, the conduction in the

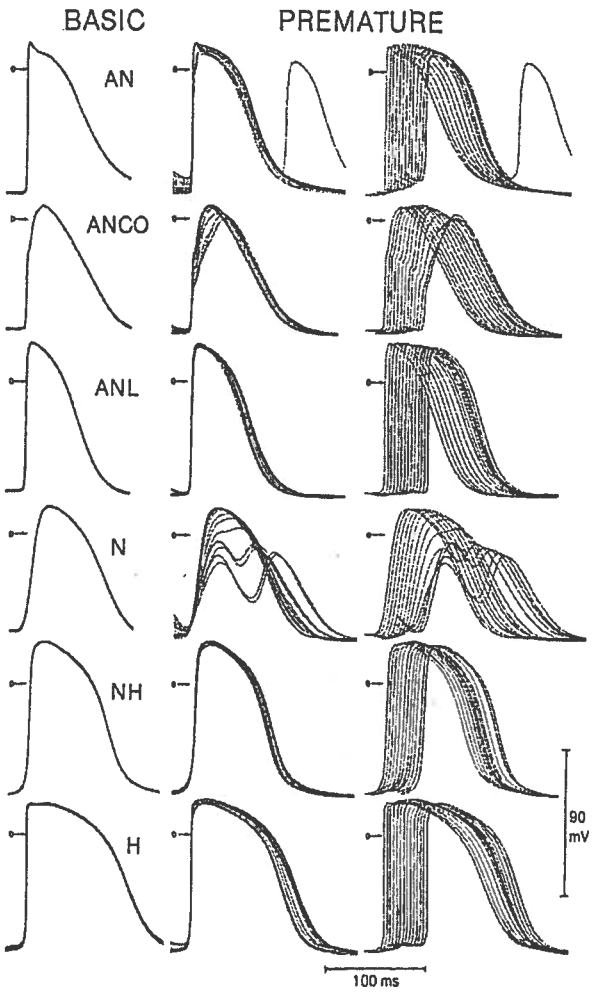

Figure III-3. Cycle-length dependent changes in transmembrane action potential characteristics at different AV nodal cells. For each of these cells, the superimposed basic action potentials (*left*) are compared with corresponding superimposed premature action potential (*center*). To facilitate their individual identification, same premature potentials are also presented with a constant rightward shift of subsequent potentials (*right*). Note for all cells similitude of action potentials obtained during basic beats, marked changes in action potential characteristics induced by premature beats, and variation of these changes with cell types. (*From Billette J: Atrioventricular nodal activation during periodic premature stimulation of the atrium. Am J Physiol 1987;252:H163-H177*)

proximal node was not a primary determinant of the concealed blocked beat. The central node (N to NH cell zone) accounts for about 50% percent of the basal delay and for the greatest fraction of its recovery-dependent increase. The distal node (NH to H cell zone) contributes about 20% of the overall nodal delay but this contribution shows a biphasic dependence on prematurity. With the decreasing recovery time, the distal conduction time first increases until it reaches a maximum at a recovery time near that at which FRPN occurs and then decreases to return to the same value at the shortest recovery time than it had at the longest one. As explained below, we suggest that this biphasic response could account for the variable shift/tilt to the left of A_2H_2 vs. A_0A_2 curves observed in the present study.

Concealed conduction tends to decrease ERPN when measured from A_0A_2, although not significantly, before slow pathway ablation. This may favour the propagation of impulses at very short coupling intervals by the central nodal cells. If an A_0 beat is conducted faster in the activated portion of the node at any given A_0A_2, this will help the test A_2 beat to be conducted faster through the same portion. When the concealed cycle length is long and the distal portion of the AV node is activated, the biphasic nature of distal delay may result in a greater contribution to the overall delay that would tend to shift back the curve to the right. Depending upon its position in the recovery cycle of distal node, a concealed A_2 beat introduced with a longer concealed cycle length could be propagated more slowly than one introduced with a short cycle length. Faster conduction may be postulated to be associated to a stronger source that will depolarized more the cells distal to the block site in the subthreshold domain. Therefore, the effects of a concealed beat on the shift/tilt to the left could be reduced with

increasing concealed cycle length. This may contribute to the reversal of the direction of the shift in longer concealed cycle length range. Further studies are obviously necessary to determine the exact origin of the biphasic nature of the tilt/shift induced by concealed conduction.

Implications

Our finding show that the concealed beat resets the excitability cycle even without producing an action potential in the zone distal to the block indicates that electrotonic interaction play a critical role in the effects of concealed conduction. In order for a neuron to fire, there are two types of electrical potentials produced. The first is a non-propagated local potential called an electrotonic potential and the second is a propagated impulse called an action potential. Small short neurons, such as those in the brain, have only electrotonic potentials while longer neurons require both. The diameter of AV nodal cells, especially those of the compact node, is very small. By analogy, a similar phenomenon may occur in small nodal cells during concealed conduction and play a critical role in excitability resetting. Clearly, the N and NH cells are electrotonically connected[38] but the specific role of this connection during concealed conduction remains to be more directly documented with microelectrode recordings.

REFERENCES

1. Tawara S: *Das Reizleitungssystem des Säugetierherzens: Eine Anatomishch-histologische Studie über das Atrioventrikularbündel und die Purkinjeschen Fäden.* Jena, Verlag von Gustav Fisher, 1906,
2. Billette J, Giles WR: Electrophysiology of the atrioventricular node; conduction, refractoriness, and ionic current. In Dangman KH, Miura DS, eds: *Electrophysiology and Pharmacology of the Heart; A Clinical Guide.* Marcel Dekker, Inc., New York, 1991, pp 141-160.
3. Zipes DP: The atrioventricular node: A riddle wrapped in a mystery inside an enigma. In Mazgalev TN, Tchou PJ, eds: *Atrial-AV Nodal Electrophysiology: A View from the Millennium.* Futura Publishing Co., Inc, Armonk, NY, 2000, pp xi-xiv.
4. Haissaguerre M, Gaita F, Fischer B, Commenges D, Montserrat P, d'Ivernois C, Lemetayer P, Warin JF: Elimination of atrioventricular nodal reentrant tachycardia using discrete slow potentials to guide application of radiofrequency energy. Circulation 1992;85:2162-2175.
5. Jackman WM, Beckman KJ, McClelland JH, Wang X, Friday KJ, Roman CA, Moulton KP, Twidale N, Hazlitt HA, Prior MI: Treatment of supraventricular tachycardia due to atrioventricular nodal reentry, by radiofrequency catheter ablation of slow-pathway conduction. N Engl J Med 1992;327:313-318.
6. Childers R: The AV node: normal and abnormal physiology. Prog Cardiovasc Dis 1977;19:361-384.

7. Levy MN, Martin PJ, Zieske H, Adler D: Role of positive feedback in the atrioventricular nodal Wenckebach phenomenon. Circ Res 1974;34:697-710.
8. Lewis T, Master AM: Observations upon conduction in the mammalian heart. A-V conduction. Heart 1925;12:209-269.
9. Merideth J, Mendez C, Mueller WJ, Moe GK: Electrical excitability of atrioventricular nodal cells. Circ Res 1968;23:69-85.
10. Billette J, Shrier A: Atrioventricular nodal activation and functional properties. In Zipes DP, Jalife J, eds: *Cardiac Electrophysiology: From Cell to Bedside.* Saunders, Philadelphia, 1995, pp 216-228.
11. Billette J: Short time constant for rate-dependent changes of atrioventricular conduction in dogs. Am J Physiol 1981;241:H26-H33.
12. Billette J, Gossard JP, Lepanto L, Cartier R: Common functional origin for simple and complex responses of atrioventricular node in dogs. Am J Physiol 1986;251:H920-H925.
13. Billette J, Metayer R, St Vincent M: Selective functional characteristics of rate-induced fatigue in rabbit atrioventricular node. Circ Res 1988;62:790-799.
14. Billette J, Metayer R: Origin, domain, and dynamics of rate-induced variations of functional refractory period in rabbit atrioventricular node. Circ Res 1989;65:164-175.
15. Medkour D, Becker AE, Khalife K, Billette J: Anatomic and functional characteristics of a slow posterior AV nodal pathway: role in dual-pathway physiology and reentry. Circulation 1998;98:164-174.

16. Khalife K, Billette J, Medkour D, Martel K, Tremblay M, Wang J, Lin LJ: Role of the compact node and its posterior extension in normal atrioventricular nodal conduction, refractory, and dual pathway properties. J Cardiovasc Electrophysiol 1999;10:1439-1451.

17. Lin LJ, Billette J, Khalife K, Martel K, Wang J, Medkour D: Characteristics, circuit, mechanism, and ablation of reentry in the rabbit atrioventricular node. J Cardiovasc Electrophysiol 1999;10:954-964.

18. Lin LJ, Billette J, Medkour D, Reid MC, Tremblay M, Khalife K: Properties and substrate of slow pathway exposed with a compact node targeted fast pathway ablation in rabbit atrioventricular node. J Cardiovasc Electrophysiol 2001;12:479-486.

19. Reid MC, Billette J, Khalife K, Tadros R: Role of compact node and posterior extension in direction-dependent changes in atrioventricular nodal function in rabbit. J Cardiovasc Electrophysiol 2003;14:1342-1350.

20. Moe GK, Abildskov JA: Observations on the ventricular dysrhythmia associated with atrial fibrillation in the dog heart. Circ Res 1964;14:447-460.

21. Moore EN: Observations on concealed conduction in atrial fibrillation. Circ Res 1967;21:201-208.

22. Hashida E, Tasaki T: Considerations on the nature of irregularity of the sequence of RR intervals and the function of the atrioventricular node in atrial fibrillation in man based on time series analysis. Jpn Heart J 1984;25:669-687.

23. Wu D, Yeh SJ, Wang CC, Wen MS, Chang HJ, Lin FC: Nature of dual atrioventricular node pathways and the tachycardia circuit as defined by radiofrequency ablation technique. J Anat 1992;20:884.

24. Billette J: What is the atrioventricular node? Some clues in sorting out its structure-function relationship. J Cardiovasc Electrophysiol 2002;13:515-518.

25. Efimov IR, Nikolski VP: Mechanisms of AV nodal excitability and propagation. In Zipes DP, Jalife J, eds: *Cardiac Electrophysiology From Cell to Bedside.* Saunders, Philadelphia, 2004, pp 203-212.

26. Meijler FL, Janse MJ: Morphology and electrophysiology of the mammalian atrioventricular node. Physiol Rev 1988;68:608-647.

27. Scherf D, J Cohen: *The Atrioventricular Node and Selected Cardiac Arrhythmias.* New York, Grune & Stratton, 1964, pp 21-46.

28. Anderson RH, Becker AE, Brechenmacher C, Davies MJ, Rossi L: The human atrioventricular junctional area. A morphological study of the A-V node and bundle. Eur J Cardiol 1975;3:11-25.

29. Titus JL, Daugherty GW, Edwards JE: Anatomy of the normal human atrioventricular conduction system. Am J Anat 1963;113:407-415.

30. Koch W: Ueber die Blutversorgung des Sinusknotens und etwaige Beziehungen des letzeren zum Atrioventrikularknoten. Muenchen Med Wchschr 1909;56:2362.

31. Woods WT, Sherf L, James TN: Structure and function of specific regions in the canine atrioventricular node. Am J Physiol 1982;243:H41-H50.

32. James TN: Anatomy of the cardiac conduction system in the rabbit. Circ Res 1967;20:638-648.

33. Ko YS, Yeh HI, Ko YL, Hsu YC, Chen CF, Wu S, Lee YS, Severs NJ: Three-dimensional reconstruction of the rabbit atrioventricular conduction axis by combining histological, desmin, and connexin mapping data. Circulation 2004;109:1172-1179.

34. Janse MJ, van Capelle FJL, Anderson RH, Touboul P, Billette J: Electrophysiology and structure of the atrioventricular node of the isolated rabbit heart. In Wellens HJJ, Lie KI, Janse MJ, eds: *The Conduction System of the Heart.* Stenfert Kroese, Leiden, The Netherlands, 1976, pp 296-315.

35. Paes de Carvalho A, de Almeida DF: Spread of activity through the atrioventricular node. Circ Res 1960;8:801-809.

36. Anderson RH, Janse MJ, van Capelle FJL, Billette J, Becker AE, Durrer D: A combined morphological and electrophysiological study of the atrioventricular node of the rabbit heart. Circ Res 1974;35:909-922.

37. Billette J, Janse MJ, van Capelle FJ, Anderson RH, Touboul P, Durrer D: Cycle-length-dependent properties of AV nodal activation in rabbit hearts. Am J Physiol 1976;231:1129-1139.

38. Billette J: Atrioventricular nodal activation during periodic premature stimulation of the atrium. Am J Physiol 1987;252:H163-H177.

39. Anderson RH: Histologic and histochemical evidence concerning the presence of morphologically distinct cellular zones within the rabbit atrioventricular node. Anat Rec 1972;173:7-23.

40. van Capelle FJL, Janse MJ, Varghese PJ, Freud GE, Mater C, Durrer D: Spread of excitation in the atrioventricular node of isolated rabbit hearts studied by multiple microelectrode recording. Circ Res 1972;31:602-616.

41. Inoue S, Becker AE: Posterior extensions of the human compact atrioventricular node: a neglected anatomic feature of potential clinical significance. Circulation 1998;97:188-193.

42. James TN: Morphology of the human atrioventricular node, with remarks pertinent to its electrophysiology. Am Heart J 1961;62:756-771.

43. Kennel AJ, Titus JL: The vasculature of the human atrioventricular conduction system. Mayo Clin Proc 1972;47:562-566.

44. Schauerte P, Scherlag BJ, Scherlag MA, Goli S, Jackman WM, Lazzara R: Ventricular rate control during atrial fibrillation by cardiac parasympathetic nerve stimulation: a transvenous approach. J Anat 1999;34:2043-2050.

45. Schauerte PN, Scherlag BJ, Scherlag MA, Goli S, Jackman W, Lazzara R: Transvenous parasympathetic cardiac nerve stimulation: an approach for stable sinus rate control. J Cardiovasc Electrophysiol 1999;10:1517-1524.

46. Schauerte P, Mischke K, Plisiene J, Waldmann M, Zarse M, Stellbrink C, Schimpf T, Knackstedt C, Sinha A, Hanrath P: Catheter stimulation of cardiac parasympathetic nerves in humans: a novel approach to the cardiac autonomic nervous system. Circulation 2001;104:2430-2435.

47. Wallick DW, Zhang Y, Tabata T, Zhuang S, Mowrey KA, Watanabe J, Greenberg NL, Grimm RA, Mazgalev TN: Selective AV nodal vagal stimulation improves

hemodynamics during acute atrial fibrillation in dogs. Am J Physiol 2001;281:H1490-H1497.

48. Zhang Y, Mowrey KA, Zhuang S, Wallick DW, Popovic ZB, Mazgalev TN: Optimal ventricular rate slowing during atrial fibrillation by feedback AV nodal-selective vagal stimulation. Am J Physiol Heart Circ Physiol 2002;282:H1102-H1110.
49. Zhang H, Mazgalev T: Achiving regular slow rhythm during atrial fibrillation without atrioventricular nodal ablation: Selective vagal stimulation plus ventricular pacing. Heart Rhythm 2004;1:469-475.
50. Hoffman BF, Paes de Carvalho A, DeMello WC, Cranefield PF: Electrical activity of single fibers of the atrioventricular node. Circ Res 1959;7:11-18.
51. Hoshino K, Anumonwo J, Delmar M, Jalife J: Wenckebach periodicity in single atrioventricular nodal cells from the rabbit heart. Circulation 1990;82:2201-2216.
52. Krayer O, Mandoki J, Mendez C: Studies on veratrum alkaloids. XVI. The action of epinephrine and of veratramine on the functional refractory period of the auriculoventricular transmission in the heartlung preparation of the dog. J Pharmacol Exp Ther 1951;105:412-419.
53. Mendez C, Moe GK: Atrioventricular transmission. In DeMello WC, ed: *Electrical Phenomena in the Heart*. Academic Press, New York, 1972, pp 263.
54. Ferrier GR, Dresel PE: Role of the atrium in determining the functional and effective refractory periods and the conductivity of the atrioventricular transmission system. Circ Res 1973;33:375-385.

55. Rosenblueth A: Functional refractory period of cardiac tissues. Am J Physiol 1958;194:171-183.

56. Denes P, Wu D, Dhingra R, Pietras RJ, Rosen KM: The effects of cycle length on cardiac refractory periods in man. Circulation 1974;49:32-41.

57. Ferrier GR, Dresel PE: Relationship of the functional refractory period to conduction in the atrioventricular node. Circ Res 1974;35:204-214.

58. Simson MB, Spear J, Moore EN: The relationship between atrioventricular nodal refractoriness and the functional refractory period in the dog. Circ Res 1979;44:121-126.

59. Cagin NA, Kunstadt D, Wolfish P, Levitt B: The influence of heart rate on the refractory period of the atrium and AV conducting system. Am Heart J 1973;85:358-366.

60. Young ML, Wolff GS, Castellanos A, Gelband H: Application of the Rosenblueth hypothesis to assess cycle length effects on the refractoriness of the atrioventricular node. Am J Cardiol 1986;57:142-145.

61. Moe GK, Mendez C, Han J: Aberrant A-V impulse propagation in the dog heart: a study of functional bundle branch block. Circ Res 1965;16:261-286.

62. Tsukada T: Effects of heart rate and isoproterenol on the functional refractory period of the AV node. Jpn J Physiol 1978;28:17-31.

63. DuBrow W, Fisher EA, Amaty-Leon G, Denes P, Wu D, Rosen K, Hastreiter AR: Comparison of cardiac refractory periods in children and adults. Circulation 1975;51:485-491.

64. Zhao J, Billette J: Beat-to-beat changes in AV nodal refractory and recovery properties during Wenckebach cycles. Am J Physiol 1992;262:H1899-H1907.

65. Tadros R, Billette J: Origin and significance of opposite effects of rate on atrioventricular nodal refractoriness. Europace Suppl 2004;6:104.

66. Sano T, Takayama N, Shimamoto T: Directional difference of conduction velocity in the cardiac ventricular syncytium studied by microelectrodes. Circ Res 1959;7:262-267.

67. Singer DH, Lazzara R, Hoffman BF: Interrelationship between automaticity and conduction in Purkinje fibers. Circ Res 1967;21:537-558.

68. Billette J, Amellal F, Zhao J, Shrier A: Relationship between different recovery curves representing rate-dependent AV nodal function in rabbit heart. J Cardiovasc Electrophysiol 1994;5:63-75.

69. Billette J: Preceding His-atrial interval as a determinant of atrioventricular nodal conduction time in the human and rabbit heart. Am J Cardiol 1976;38:889-896.

70. Moe GK, Childers RW, Merideth J: An appraisal of "supernormal" A-V conduction. Circulation 1968;38:5-28.

71. Simson MB, Spear JF, Moore EN: Electrophysiologic studies on atrioventricular nodal Wenckebach cycles. Am J Cardiol 1978;41:244-258.

72. Mobitz W: Uber die unvollstandige Storung der Erregungsuberleitung zwischen Vorhof und Kammer des menschlichen Herzens. Z Ges Exp Med 1924;41:180-237.

73. Alanis J, Gonzales H, Lopez E: The electrical activity of the bundle of His. J Physiol 1958;142:127-140.

74. Alanis J, Lopez E, Mandoki JJ, Pilar G: Propagation of impulses through the atrioventricular node. Am J Physiol 1959;197:1171-1174.

75. Hoffman BF, Cranefield PF, Stuckey JH, Bagdonas A: Electrical activity during the PR interval. Circ Res 1960;8:1200-1211.

76. Damato AN, Lau SH, Berkowitz WD, Rosen KM, Lisi KR: Recording of specialized conducting fibers (A-V nodal, His bundle, and right bundle branch) in man using an electrode catheter technic. Circulation 1969;39:435-447.

77. Giraud G, Puech P, Latour H: L'activité électrique physiologique du noeud de Tawara et du faisceau de His chez l'homme. Acad Nat Med 1960;17:363-366.

78. Kure K: Ueber die Pathogenese der heterotopen Reizbildung unter dem Einflusse der extrakardialen Herznerven. Ztschr exper Path und Ther 1913;12:389.

79. Zahn A: Experimentelle Untersuchungen ueber die Reizbildung und Reizleitung im Atrioventrikularknoten. Arch ges Physiol 1913;151:247.

80. Matsuda K, Hoshi T, Kameyama S: Action potential of the atrioventricular node (Tawara). Tohoku J Exper Med 1958;66:8.

81. Billette J, St-Vincent M: Functional origin of rate-induced changes in atrioventricular nodal conduction time of premature beats in the rabbit. Can J Physiol Pharmacol 1987;65:2329-2337.

82. Hoffman BF, PF Cranefield: *Electrophysiology of the Heart.* New York, McGraw-Hill Book Co., 1960, pp 132-174.

83. Wennemark JR, Ruesta VJ, Brody DA: Microelectrode study of delayed conduction in the canine right bundle branch. Circ Res 1968;23:753-769.

84. Jalife J, Moe GK: Excitation, conduction, and reflection of impulses in isolated bovine and serum cardiac Purkinje fibers. Circ Res 1981;49:233-247.

85. Talajic M, Papadatos D, Villemaire C, Glass L, Nattel S: A unified model of atrioventricular nodal conduction predicts dynamic changes in Wenckebach periodicity. Circ Res 1991;68:1280-1293.

86. Loeb JM, deTarnowsky JM, Whitson CC, Warner MR: Atrioventricular nodal accommodation: rate- and time-dependent effects. Am J Physiol 1987;252:H578-H584.

87. Nayebpour M, Talajic M, Villemaire C, Nattel S: Vagal modulation of the rate-dependent properties of the atrioventricular node. Circ Res 1990;67:1152-1166.

88. Nayebpour M, Talajic M, Nattel S: Quantitation of dynamic AV nodal properties and application to predict rate-dependent AV conduction. Am J Physiol 1991;261:H292-H300.

89. Billette J, Nattel S: Dynamic behavior of the atrioventricular node: a functional model of interaction between recovery, facilitation, and fatigue. J Cardiovasc Electrophysiol 1994;5:90-102.

90. Billette J, Zhao J, Shrier A: Mechanisms of conduction time hysteresis in rabbit atrioventricular node. Am J Physiol 1995;269:H1258-H1267.

91. Amellal F, Hall K, Glass L, Billette J: Alternation of atrioventricular nodal conduction time during atrioventricular reentrant tachycardia: are dual pathways necessary? J Cardiovasc Electrophysiol 1996;7:943-951.

92. Zhao J, Billette J: Characteristics and mechanisms of the effects of heart rate history on transient AV nodal responses. Am J Physiol 1996;270:H2070-H2080.

93. Lehmann MH, Steinman RT, Meissner MD, Schuger CD: Quantitating AV nodal function: has A1A2 outlived its usefulness? Pacing Clin Electrophysiol 1990;13:1674-1677.

94. Fahy GJ, Efimov I, Cheng Y, Kidwell GA, Van Wagoner D, Tchou PJ, Mazgalev T: Mechanism of atrioventricular nodal facilitation in the rabbit heart: role of the distal AV node. Am J Physiol 1997;272:H2815-H2825.

95. Mazgalev T, Mowrey K, Efimov I, Fahy GJ, Van Wagoner D, Cheng Y, Tchou PJ: Mechanism of atrioventricular nodal facilitation in rabbit heart: role of proximal AV node. Am J Physiol 1997;273:H1658-H1668.

96. Shrier A, Dubarsky H, Rosengarten M, Guevara MR, Nattel S, Glass L: Prediction of complex atrioventricular conduction rhythms in humans with use of the atrioventricular nodal recovery curve. Circulation 1987;76:1196-1205.

97. Steinman RT, Lehmann MH: Beat-to-beat changes in atrioventricular nodal excitability and its modulation by concealed conduction during functional 2:1 block in man. Circulation 1987;76:759-767.

98. Moe GK, Preston JB, Burlington H: Physiologic evidence for a dual A-V transmission system. Circ Res 1956;4:357-375.

99. Mendez C, Moe GK: Demonstration of a dual A-V nodal conduction system in the isolated rabbit heart. Circ Res 1966;19:378-393.

100. Schuilenburg RM, Durrer D: Atrial echo beats in the human heart elicited by induced atrial premature beats. Circulation 1968;37:680-693.

101. Janse MJ, Capelle FJ, Freud GE, Durrer D: Circus movement within the AV node as a basis for supraventricular tachycardia as shown by multiple microelectrode recording in the isolated rabbit heart. Circ Res 1971;28:403-414.

102. Denes P, Wu D, Dhingra RC, Chuquimia R, Rosen KM: Demonstration of dual A-V nodal pathways in patients with paroxysmal supraventricular tachycardia. Circulation 1973;48:549-555.

103. Patterson E, Scherlag BJ: Longitudinal dissociation within the posterior AV nodal input of the rabbit: a substrate for AV nodal reentry. Circulation 1999;99:143-155.

104. Ross DL, Johnson DC, Denniss AR, Cooper MJ, Richards DA, Uther JB: Curative surgery for atrioventricular junctional ("AV nodal") reentrant tachycardia. J Anat 1985;6:1383-1392.

105. Cox JL, Holman WL, Cain ME: Cryosurgical treatment of atrioventricular node reentrant tachycardia. Circulation 1987;76:1329-1336.

106. Huang SK, Bharati S, Graham AR, Lev M, Marcus FI, Odell RC: Closed chest catheter desiccation of the atrioventricular junction using radiofrequency energy--a new method of catheter ablation. J Anat 1987;9:349-358.

107. Otomo K, Wang Z, Lazzara R, Jackman WM: Atrioventricular nodal reentrant tachycardia: electrophysiologic characteristics of four forms and implications for the reentrant circuit. In Zipes DP, Jalife J, eds: *Cardiac Electrophysiology: From Cell to Bedside*. WB Saunders Co, Philadelphia, 2000, pp 504-521.

108. Haissaguerre M, Jais P, Shah DC, Hocini M, Takahashi A, Gaita F, Barold SS, Clementy J: Analysis of electrophysiological activity in Koch's triangle relevant

to ablation of the slow AV nodal pathway. Pacing Clin Electrophysiol 1997;20:2470-2481.

109. Janse MJ: Influence of the direction of the atrial wave front on A-V nodal transmission in isolated hearts of rabbits. Circ Res 1969;25:439-449.

110. Antz M, Scherlag BJ, Patterson E, Otomo K, Tondo C, Pitha J, Gonzalez MD, Jackman WM, Lazzara R: Electrophysiology of the right anterior approach to the atrioventricular node: studies in vivo and in the isolated perfused dog heart. J Cardiovasc Electrophysiol 1997;8:47-61.

111. Hirao K, Scherlag BJ, Poty H, Otomo K, Tondo C, Antz M, Patterson E, Jackman WM, Lazzara R: Electrophysiology of the atrio-AV nodal inputs and exits in the normal dog heart: radiofrequency ablation using an epicardial approach. J Cardiovasc Electrophysiol 1997;8:904-915.

112. Antz M, Scherlag BJ, Otomo K, Pitha J, Tondo C, Patterson E, Jackman WM, Lazzara R: Evidence for multiple atrio-AV nodal inputs in the normal dog heart. J Cardiovasc Electrophysiol 1998;9:395-408.

113. Ross DL, Brugada P, Bar FW, Vanagt EJ, Weiner I, Farre J, Wellens HJ: Comparison of right and left atrial stimulation in demonstration of dual atrioventricular nodal pathways and induction of intranodal reentry. Circulation 1981;64:1051-1058.

114. Jazayeri MR, Sra JS, Akhtar M: Atrioventricular nodal reentrant tachycardia. Electrophysiologic characteristics, therapeutic interventions, and specific reference to anatomic boundary of the reentrant circuit. Cardiol Clin 1993;11:151-181.

115. de Bakker JM, Loh P, Hocini M, Thibault B, Janse MJ: Double component action potentials in the posterior approach to the atrioventricular node: do they reflect activation delay in the slow pathway? J Anat 1999;34:570-577.

116. Amellal F, Billette J: Selective functional properties of dual atrioventricular nodal inputs. Role in nodal conduction, refractoriness, summation, and rate-dependent function in rabbit heart. Circulation 1996;94:824-832.

117. Wu J: Nondiscrete functional pathways and asymmetric transitional zone: a new concept for AV nodal electrophysiology. J Cardiovasc Electrophysiol 2001;12:487-488.

118. Nikolski V, Efimov IR: Fluorescent imaging of a dual-pathway atrioventricular-nodal conduction system. Circ Res 2001;88:E23-E30.

119. Nikolski VP, Jones SA, Lancaster MK, Boyett MR, Efimov IR: Cx43 and dual-pathway electrophysiology of the atrioventricular node and atrioventricular nodal reentry. Circ Res 2003;92:469-475.

120. Josephson ME: *Clinical Cardiac Electrophysiology: Techniques and Interpretation.* Philadelphia, Lea & Febiger, 1993, pp 22-70.

121. Sheahan RG, Klein GJ, Yee R, Le Feuvre CA, Krahn AD: Atrioventricular node reentry with 'smooth' AV node function curves: a different arrhythmia substrate? Circulation 1996;93:969-972.

122. Tai CT, Chen SA, Chiang CE, Lee SH, Wen ZC, Chiou CW, Ueng KC, Chen YJ, Yu WC, Huang JL, Chang MS: Complex electrophysiological characteristics in atrioventricular nodal reentrant tachycardia with continuous atrioventricular node function curves. Circulation 1997;95:2541-2547.

123. Mazgalev TN, Tchou PJ: The AV nodal dual pathway electrophysiology: still a controversial concept. In Mazgalev TN, Tchou PJ, eds: *Atrial-AV Nodal Electrophysiology: A View from the Millennium*. Futura Publishing Co., Inc, Armonk, NY, 2000, pp 217-236.

124. Engelmann TW: Beobachtungen une versuche an suspendirten herzen. Pflugers Arch 1894;56:149-202.

125. Ashman R: Conductivity in compressed cardiac muscle. I. The recovery of conductivity following impulse transmission in compressed auricular muscle of the turtle heart. Am J Physiol 1925;74:121-139.

126. Langendorf R: Concealed A-V conduction: The effect of blocked impulses on the formation and conduction of subsequent impulses. Am Heart J 1948;35:542-552.

127. Billette J: Anatomy and physiology of concealment in dual atrioventricular nodal pathways. J Cardiovasc Electrophysiol 2004;15:150-152.

128. Langendorf R, Pick A, Edelist A, Katz LN: Experimental demonstration of concealed AV conduction in the human heart. Circulation 1965;32:386-393.

129. Yamada K, Okajima M, Hori K, Fujino T, Muraki H, Hishida H, Kobayashi T: On the genesis of the absolute ventricular arrhythmia associated with atrial fibrillation. Circ Res 1968;22:707-715.

130. Langendorf R, Pick A, Katz LN: Ventricular response in atrial fibrillation. Role of condealed conduction in the A-V junction. Circulation 1965;32:69-75.

131. Chorro FJ, Sanchis J, Lopez-Merino V, Such L, Avellana JA, Valentin V: Effects of atrial impulse timing on AV concealed conduction in the rabbit heart. Pacing Clin Electrophysiol 1991;14:842-853.

132. Liu S, Olsson SB, Yang Y, Hertervig E, Kongstad O, Yuan S: Concealed conduction and dual pathway physiology of the atrioventricular node. J Cardiovasc Electrophysiol 2004;15:144-149.

133. Moore EN: Microelectrode studies on concealment of multiple premature atrial responses. Circ Res 1966;18:660-672.

134. Watanabe Y, Watanabe M: Impulse formation and conduction of excitation in the atrioventricular node. J Cardiovasc Electrophysiol 1994;5:517-531.

135. Billette J, Nadeau RA, Roberge F: Relation between the minimum RR interval during atrial fibrillation and the functional refractory period of the AV junction. Cardiovasc Res 1974;8:347-351.

136. Scherf D, Schott A: *Extrasystoles and Allied Arrhythmias*. Chicago, William Heinemann Medical Books, Ltd, 1973, pp 561.

137. Hoffman BF: Electrical activity of the atrio-ventricular node. In Paes de Carvalho A, de Mello WC, Hoffman BF, eds: *The Specialized Tissue of the Heart*. Amsterdam, 1961, pp 143-158.

138. Meijler FL, Fisch C: Does the atrioventricular node conduct? Brit Heart J 1989;61:309-315.

139. Jalife J, Moe GK: Effect of electrotonic potentials on pacemaker activity of canine Purkinje fibers in relation to parasystole. Circ Res 1976;39:801-808.

140. Meijler FL, Jalife J, Beaumont J, Vaidya D: AV nodal function during atrial fibrillation: the role of electrotonic modulation of propagation. J Cardiovasc Electrophysiol 1996;7:843-861.

141. West TC, Toda N: Response of the A-V node of the rabbit to stimulation of intracardiac cholinergic nerves. Circ Res 1967;20:18-31.

142. Zipes DP, Mendez C, Moe GK: Some examples of Wenckebach periodicity in cardiac tissues, with an appraisal of mechanisms. In Rosenbaum MB, Elizar MV, eds: *The Frontiers of Cardiac Electrophysiology*. Martinus Nijhoff, Boston, 1983, pp 357-375.

143. Mazgalev T, Dreifus LS, Michelson EL: A new mechanism for atrioventricular nodal gap-vagal modulation of conduction. Circulation 1989;79:417-430.

144. Lewis T: *The mecanism and Graphic Registration of the Heart Beat*. London, Shaw & Sons, 1925, pp 377.

145. van der Tweel LH, Meijler FL, van Capelle FJ: Synchronization of the heart. J Appl Physiol 1973;34:283-287.

146. Cohen RJ, Berger RD, Dushane TE: A quantitative model for the ventricular response during atrial fibrillation. IEEE Trans Biomed Eng 1983;30:769-781.

147. Meijler FL, Strackee J, Stokhof AA, Wassenaar C: Scaling of atrioventricular transmission in mammalian species: an evolutionary riddle! J Cardiovasc Electrophysiol 2002;13:826-830.

148. Wennemark JR, Bandura JP, Brody DA, Ruesta VJ: Microelectrode study of high grade block in canine Purkinje fibers. J Electrocardiol 1975;8:299-306.

149. Antzelevitch C, Moe GK: Electrotonic inhibition and summation of impulse conduction in mammalian Purkinje fibers. Am J Physiol 1983;245:H42-H53.

150. Davidenko JM, Delmar M, Beaumont J, Michaels DC, Lorente P, Jalife J: Electrotonic inhibition and active facilitation of excitability in ventricular muscle. J Cardiovasc Electrophysiol 1994;5:945-960.

151. Liu Y, Zeng W, Delmar M, Jalife J: Ionic mechanisms of electronic inhibition and concealed conduction in rabbit atrioventricular nodal myocytes. Circulation 1993;88:1634-1646.

152. Lee PC, Wu JM, Wolff GS, Young ML: Effects of a blocked atrial beat on the atrioventricular nodal recovery property in patients with dual nodal pathways. Pacing Clin Electrophysiol 2003;26:2091-2095.

153. Wu D, Denes P, Dhingra RC, Wyndham CR, Rosen KM: Quantification of human atrioventricular nodal concealed conduction utilizing S1S2S3 stimulation. Circ Res 1976;39:659-665.

154. Fujiki A, Tani M, Mizumaki K, Yoshida S, Sasayama S: Quantification of human concealed atrioventricular nodal conduction: relation to ventricular response during atrial fibrillation. Am Heart J 1990;120:598-603.

155. Antzelevitch C, Moe GK: Electrotonic inhibition and summation of impulse conduction in mammalian Purkinje fibers. Am J Physiol 1983;245:H42-H53.

156. McKinnie J, Avitall B, Caceres J, Jazayeri M, Tchou P, Akhtar M: Electrophysiologic spectrum of concealed intranodal conduction during atrial rate acceleration in a model of 2:1 atrioventricular block. Circulation 1989;80:43-50.